Supporting Information

Switching between Photochromism and Photoluminescence in Schiff Base Derivatives by Molecular Design of End Groups

Qilong Zhang,[a, b, ‡, *] Xu Zhou,[a, ‡] Xiaofeng Shan,[a, ‡] Fa He,[b] Yuwei Bao,[a] Hong Xu,[a] Chun Zhu,[b, *] Bixue Zhu[b, *]

[a] School of Basic Medical Sciences, Guizhou Key Laboratory of Macrocyclic and Supramolecular Chemistry, Guizhou Medical University, Guiyang 561113, PR China

[b] Guizhou Key Laboratory of Macrocyclic and Supramolecular Chemistry, School of Chemistry and Chemical Engineering, Guizhou University, Guiyang 550025, PR China

* Corresponding author

E-mail:gzuqlzhang@126.com

czhu2014@163.com

bxzhu@gzu.edu.cn

‡ The authors contributed equally to this study.

Table of Contents

1. Experimental Section

1.1 Materials and instrumentation.

All chemical materials used in this study were obtained from commercial suppliers and were not further purified. ESI-TOF mass spectra were obtained with an Agilent HPLC-6545. 1H/13C NMR spectra were measured on a Bruker Avance III, and chemical shifts are reported in ppm (in DMSO-d6, TMS is the internal standard). Ultraviolet absorption spectra were measured using a Shimadzu UV-2600 ultraviolet absorption spectrophotometer.Fluorescence emission spectroscopy was performed on a Cary eclipse fluorescence spectrometer from Varian, USA. X-ray crystallography was performed on a Bruker APEX III diffractometer. The powder X-ray diffraction patterns were recorded on a Bruker D8 Advance diffractometer.

1.2 Mono-molecular theory UV-visible absorption spectroscopy calculations.

In the computational simulation performed using the ORCA quantum chemistry software (Version 6.0.0) [Neese, F. Software update: The ORCA program system—Version 5.0. WIREs Comput Mol Sci. 2022;e1606. https://doi.org/10.1002/wcms.1606], we employed the wb97x-d3 functional[Y.-S. Lin, G.-D. Li, S.-P. Mao, and J.-D. Chai. Long-range corrected hybrid density functionals with improved dispersion corrections. J. Chem. Theory Comput., 9:263–272, 2013.] in conjunction with the def2-SVP basis set[F. Weigend and R. Ahlrichs, Phys. Chem. Chem. Phys. 7, 3297 (2005)] to conduct excited state calculations. The wb97x-d3 functional is Range-separated hybrid functional that provides a balanced approach to describing both ground and excited state properties.

2. Synthesis procedures

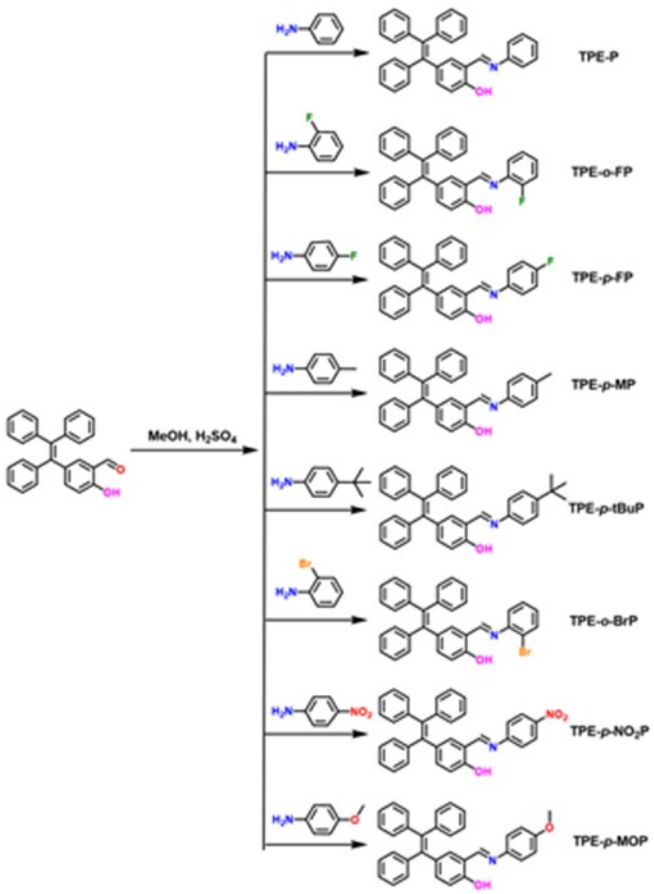

Scheme S1. Synthesis route of the compounds.

TPE-P: 2-hydroxy-5-(1,2,2-triphenylvinyl)benzaldehyde (0.38 g, 1 mmol) and aniline (0.12 g, 1.2 mmol) were dissolved in 20 mL ethanol. 20 μL concentrated sulfuric acid was added dropwise, and the mixture reacted overnight at room temperature. The mixture was filtered, and the solid was washed with ethanol and dried to afford the target product. Compounds **TPE-*p*-tBuP**, **TPE-*o*-FP**, **TPE-*p*-FP**, **TPE-*p*-MP**, **TPE-*p*-MOP**, **TPE-*o*-BrP**, and **TPE-*p*-NO_2P** were synthesized by reacting 2-hydroxy-5-(1,2,2-triphenylvinyl)benzaldehyde with 4-tert-butylaniline, 2-fluoroaniline, 4-fluoroaniline, 4-methylaniline, 2-methoxyaniline, 2-bromoaniline, and 4-nitroaniline (**Scheme S1**).

3. Spectroscopic characterization data of the compound

TPE-P: m.p. 171℃; ^{1}H NMR (600 MHz, DMSO-d_6) δ 13.10 (s, 1H), 8.75 (s, 1H), 7.42 (t, J = 7.8 Hz, 2H), 7.35 (d, J = 7.4 Hz, 2H), 7.28 (dd, J = 13.2, 4.8 Hz, 2H), 7.19 – 7.07 (m, 10H), 7.03 – 6.95 (m, 6H), 6.72 (d, J = 8.5 Hz, 1H) ppm. ^{13}C NMR (151 MHz, DMSO-d_6) δ 163.09, 159.09, 147.89, 143.30, 143.04, 140.36, 139.66, 135.89, 134.45, 134.22, 130.81, 130.74, 130.70, 129.46, 128.92, 128.00, 127.94, 127.88, 127.01, 126.71, 126.57, 126.52, 121.39, 118.84, 116.20 ppm. ESI-TOF：$[M+H]^+$ calcd for $C_{33}H_{26}NO^+$: 452.1936, found 452.2040.

TPE-*o*-FP: m.p. 162℃; ^{1}H NMR (600 MHz, DMSO-d_6) δ 13.23 (s, 0.5H), 12.93 (s, 0.5H), 8.74 (s, 1H), 7.42 (dd, J = 8.9, 5.0 Hz, 1H), 7.24 (ddd, J = 16.3, 12.6, 8.4 Hz, 4H), 7.19 – 7.07 (m, 9H), 6.99 (ddd, J = 19.4, 13.5, 6.9 Hz, 7H), 6.71 (dd, J = 8.5, 6.0 Hz, 1H) ppm. ^{13}C NMR (151 MHz, DMSO-d_6) δ 163.01, 162.16, 160.20, 159.09, 158.94, 145.18, 144.41, 143.29, 143.05, 140.37, 140.31, 139.69, 139.64, 136.60, 135.89, 135.68, 134.38, 134.26, 134.17, 130.80, 130.74, 130.70, 129.95, 127.99, 127.93, 127.87, 126.70, 126.57, 126.52, 123.32, 123.26, 121.25, 118.84, 116.22, 116.18, 116.15, 116.07, 115.65, 115.51, 20.64 ppm. ESI-TOF：$[M+H]^+$ calcd for $C_{33}H_{25}FNO^+$: 470.1842, found 470.1900.

TPE-*p*-FP: m.p. 175℃; ^{1}H NMR (600 MHz, DMSO-d_6) δ 13.02 (s, 1H), 8.85 (s, 1H), 7.51 (t, J = 8.0 Hz, 1H), 7.34 – 7.27 (m, 3H), 7.26 – 7.21 (m, 1H), 7.19 – 7.07 (m, 9H), 7.02 (dd, J = 13.2, 6.5 Hz, 5H), 6.97 (d, J = 6.8 Hz, 2H), 6.73 (d, J = 8.5 Hz, 1H) ppm. ^{13}C NMR (151 MHz, DMSO-d_6) δ 164.44, 159.19, 156.25, 154.61, 143.27, 143.01, 140.44, 139.56, 136.36, 135.73, 135.67, 134.46, 134.34, 130.81, 130.74, 130.69, 128.46, 128.40, 128.02, 127.95, 127.87, 126.73, 126.60, 126.54, 125.19, 125.16, 120.71, 118.87, 116.39, 116.32, 116.26, 39.60 ppm. ESI-TOF：$[M+H]^+$ calcd for $C_{33}H_{25}FNO^+$: 470.1842, found 470.1932.

TPE-*p*-MP: m.p. 167℃; ^{1}H NMR (600 MHz, DMSO-d_6) δ 13.33 (s, 1H), 8.72 (s, 1H), 7.36 (d, J = 8.9 Hz, 2H), 7.21 (d, J = 2.2 Hz, 1H), 7.13 (ddd, J = 21.3, 15.4, 7.1 Hz, 9H), 7.01 (t, J = 7.3 Hz, 4H), 6.99 – 6.94 (m, 5H), 6.69 (d, J = 8.5 Hz, 1H), 3.77 (s, 3H) ppm. ^{13}C NMR (151 MHz, DMSO-d_6) δ 160.82, 158.98, 158.58, 143.33, 143.08, 140.53, 140.27, 139.73, 135.37, 134.25, 134.12, 130.80, 130.74, 130.70, 127.98, 127.92, 127.86, 126.68, 126.54, 122.66, 118.92, 116.09, 114.66, 55.42 ppm. ESI-TOF：$[M+H]^+$ calcd for $C_{34}H_{28}NO^+$: 466.2093, found 466.2189.

TPE-*p*-tBuP: m.p. 215℃; ^{1}H NMR (600 MHz, DMSO-d_6) δ 13.26 (s, 1H), 8.74 (s,1H), 7.43 (d, J = 8.5 Hz, 2H), 7.29 (d, J = 8.5 Hz, 2H), 7.24 (d, J = 2.0 Hz, 1H), 7.13 (ddq, J = 29.3, 14.5, 7.3 Hz, 10H), 7.04 – 6.93 (m, 6H), 6.71 (d, J = 8.5 Hz, 1H), 1.28 (s, 9H) ppm. ^{13}C NMR (151 MHz, DMSO-d_6) δ 162.39, 159.12, 149.74, 145.16, 143.31, 143.04, 140.33, 139.68, 135.71, 134.39, 134.15, 130.81, 130.73, 130.69, 128.00, 127.94, 127.88, 126.71, 126.56, 126.52, 126.20, 121.02, 118.85, 116.17, 34.36, 31.16 ppm.ESI-TOF：$[M+H]^+$ calcd for $C_{37}H_{34}NO^+$: 508.2652, found 508.2659.

TPE-*p*-MOP: m.p. 120℃; ^{1}H NMR (600 MHz, DMSO-d_6) δ 13.24 (s, 1H), 8.74 (s, 1H), 7.24 (dt, J = 14.2, 8.3 Hz, 5H), 7.19 – 7.07 (m, 9H), 7.04 – 6.94 (m, 7H), 6.70 (d, J = 8.5 Hz, 1H), 2.31 (s, 9H) ppm. ^{13}C NMR (151 MHz, DMSO-d_6) δ 162.16, 159.09, 145.19, 143.31, 143.05, 140.31, 139.69, 136.59, 135.67, 134.38, 134.17, 130.80, 130.74, 130.70, 129.94, 127.98, 127.93, 127.87, 126.69, 126.55, 121.25, 118.84, 116.15, 20.64 ppm. ESI-TOF：$[M+H]^+$ calcd for $C_{34}H_{28}NO_2^+$: 482.2042, found 482.2141.

TPE-*o*-BrP: m.p. 216℃; ^{1}H NMR (600 MHz, DMSO-d_6) δ 13.05 (s, 1H), 8.79 (s, 1H), 7.73 (d, J = 7.9 Hz, 1H), 7.52 (d, J = 8.0 Hz, 1H), 7.44 (t, J = 7.2 Hz, 1H), 7.29 (d, J = 2.1 Hz, 1H), 7.20 – 7.09 (m, 10H), 7.06 – 7.00 (m, 5H), 6.97 (d, J = 7.0 Hz, 2H), 6.74 (d, J = 8.5 Hz, 1H) ppm. ^{13}C NMR (151 MHz, DMSO-d_6) δ 164.30, 159.17, 145.84, 143.28, 143.24, 143.00, 140.46, 139.52, 136.48, 134.92, 134.37, 132.94,

130.81, 130.74, 130.69, 129.03, 128.59, 128.04, 127.96, 127.88, 126.73, 126.62, 126.54, 120.03, 119.43, 118.66, 116.33 ppm. ESI-TOF：$[M+H]^+$ calcd for $C_{33}H_{25}BrNO^+$: 530.1041, found 530.1141.

TPE-*p*-NO_2P: m.p. 241℃; ^{1}H NMR (600 MHz, DMSO-d_6) δ 12.26 (s, 1H), 8.82 (s, 1H), 8.26 (d, J = 9.0 Hz, 2H), 7.53 (d, J = 9.0 Hz, 2H), 7.35 (d, J = 2.3 Hz, 1H), 7.13 (tdt, J = 21.3, 14.3, 7.3 Hz, 10H), 7.05 (dd, J = 8.6, 2.3 Hz, 1H), 7.02 (dd, J = 9.6, 4.3 Hz, 4H), 6.99 – 6.93 (m, 2H), 6.74 (d, J = 8.6 Hz, 1H) ppm. ^{13}C NMR (151 MHz, DMSO-d_6) δ 165.11, 159.04, 154.55, 145.44, 143.24, 142.97, 140.52, 139.50, 136.92, 134.53, 134.12, 130.79, 130.74, 130.68, 128.03, 127.97, 127.88, 126.74, 126.62, 126.55, 125.04, 122.51, 119.06, 116.36 ppm. ESI-TOF：$[M+H]^+$ calcd for $C_{33}H_{25}N_2O_3^+$: 497.1787, found 497.1868.

4. Preparation of Color-Changing Ink.

Grind the compound powder with castor oil (1:4 ratio) until the mixture reaches a state where “the oil does not float and the powder does not settle.” Finally, add mugwort wool in batches and stir until a soft paste forms. Store in sealed glass containers.

5. TOF-MS Spectra

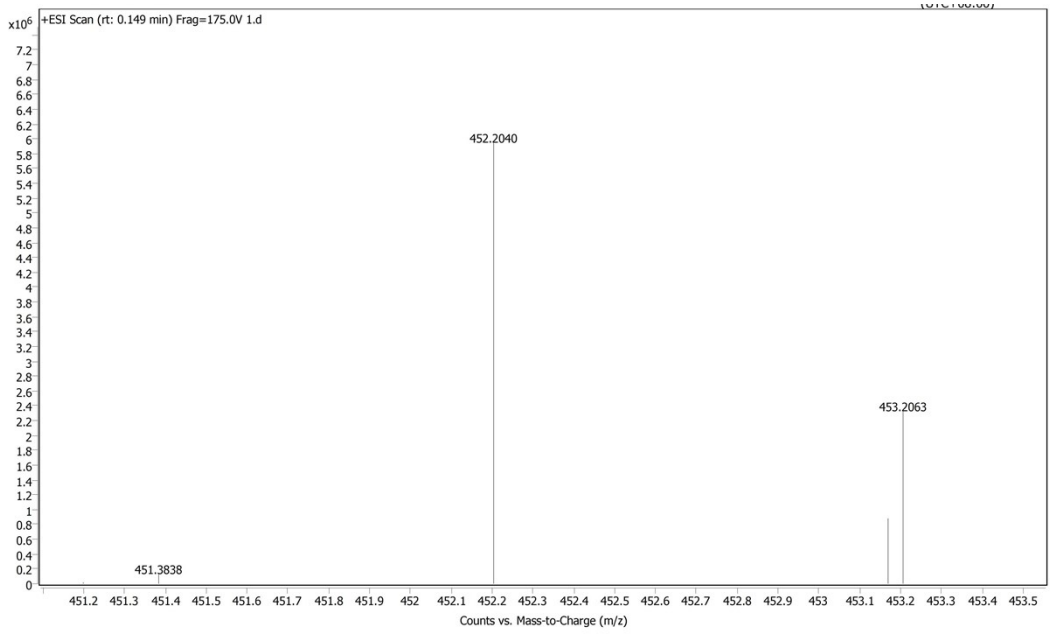

Figure S1. MS spectrum of **TPE-P**.

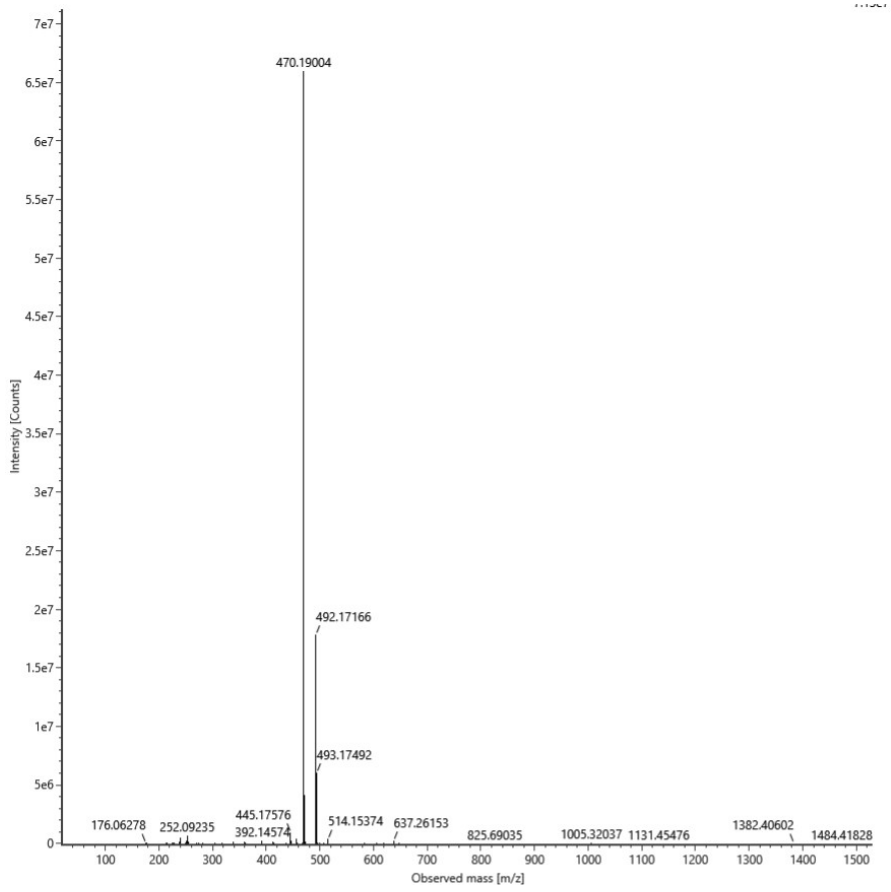

Figure S2. MS spectrum of **TPE-*o*-FP**.

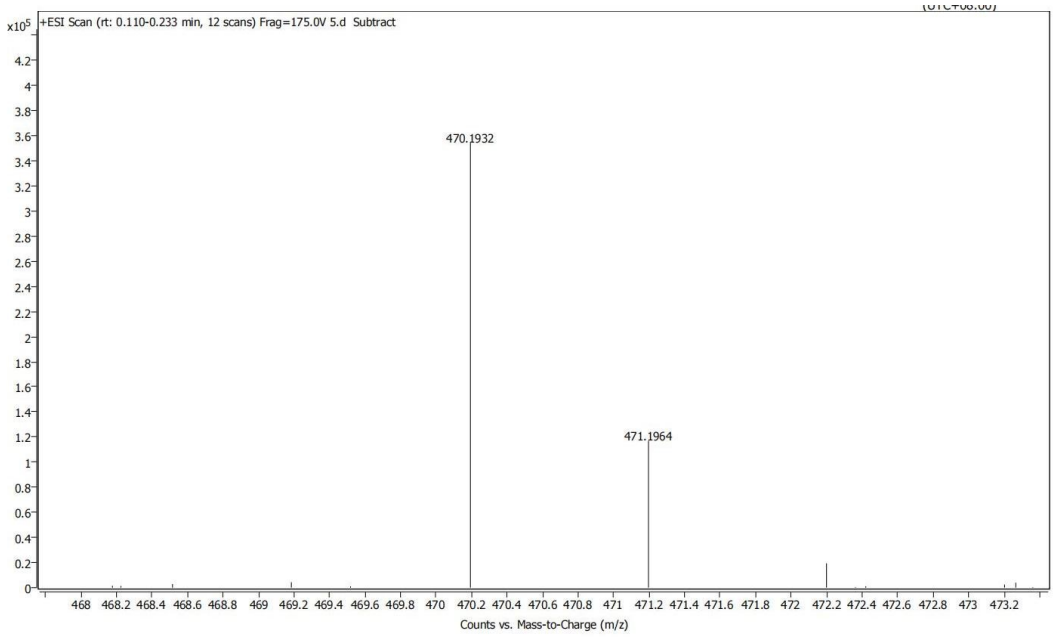

Figure S3. MS spectrum of **TPE-*p*-FP**.

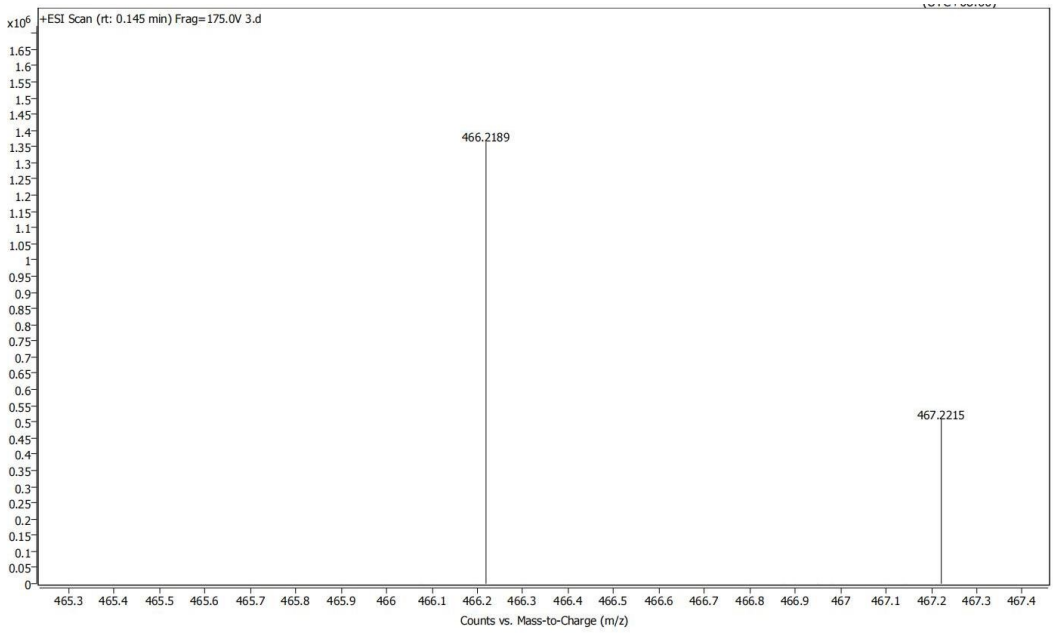

Figure S4. MS spectrum of **TPE-*p*-MP**.

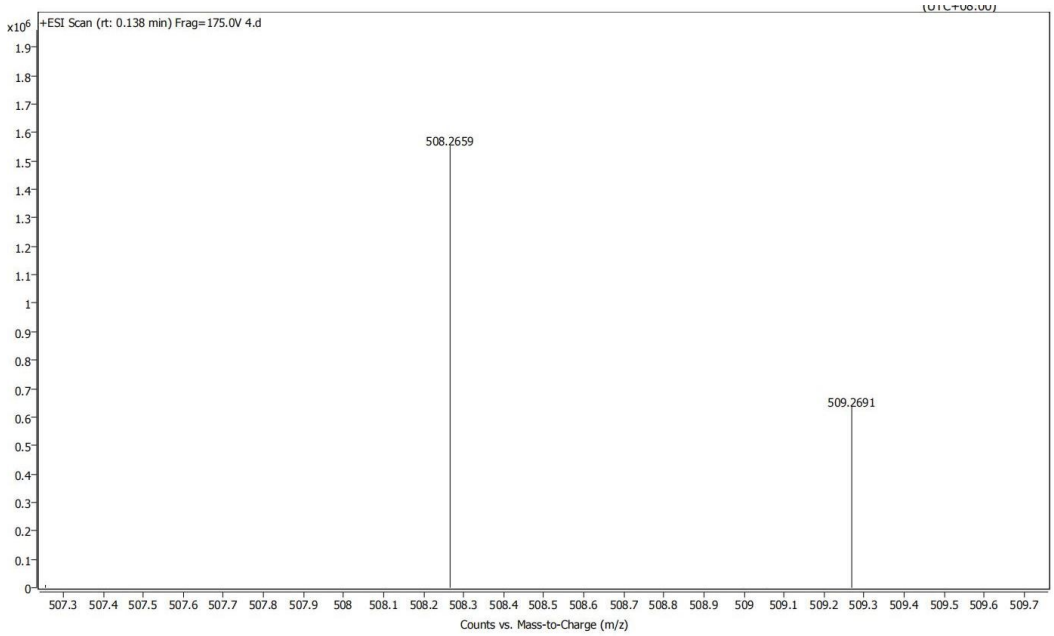

Figure S5. MS spectrum of **TPE-*p*-tBuP**.

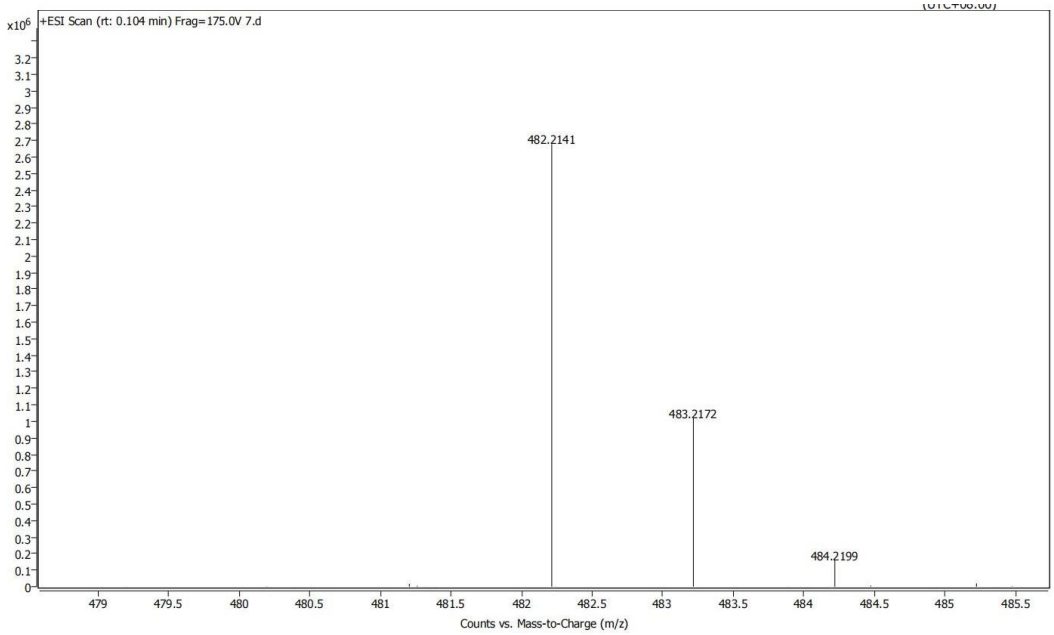

Figure S6. MS spectrum of **TPE-*p*-MOP**.

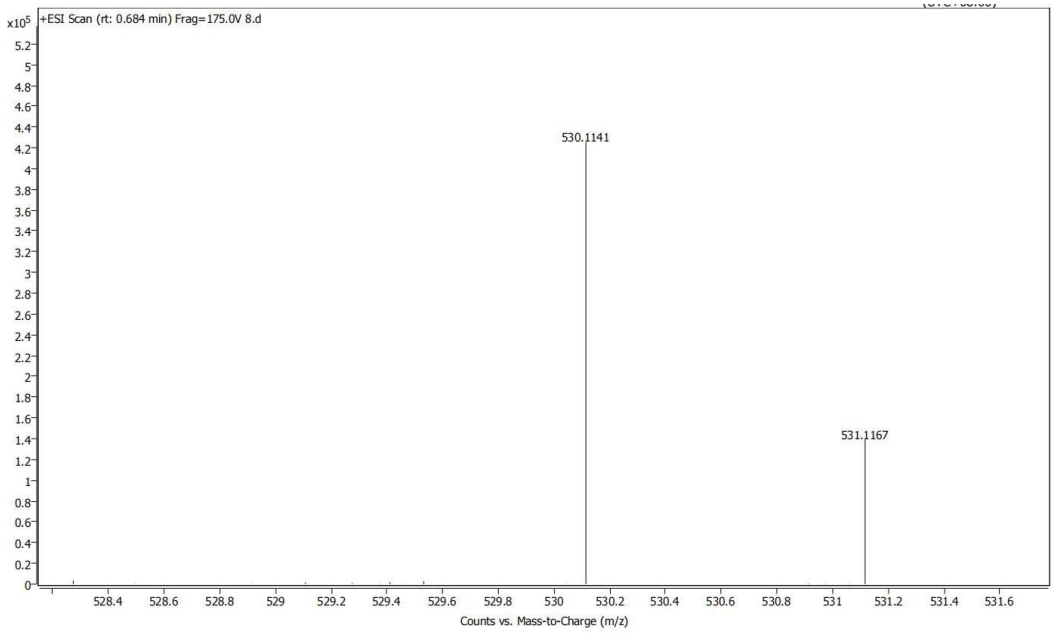

Figure S7. MS spectrum of **TPE-*o*-BrP**.

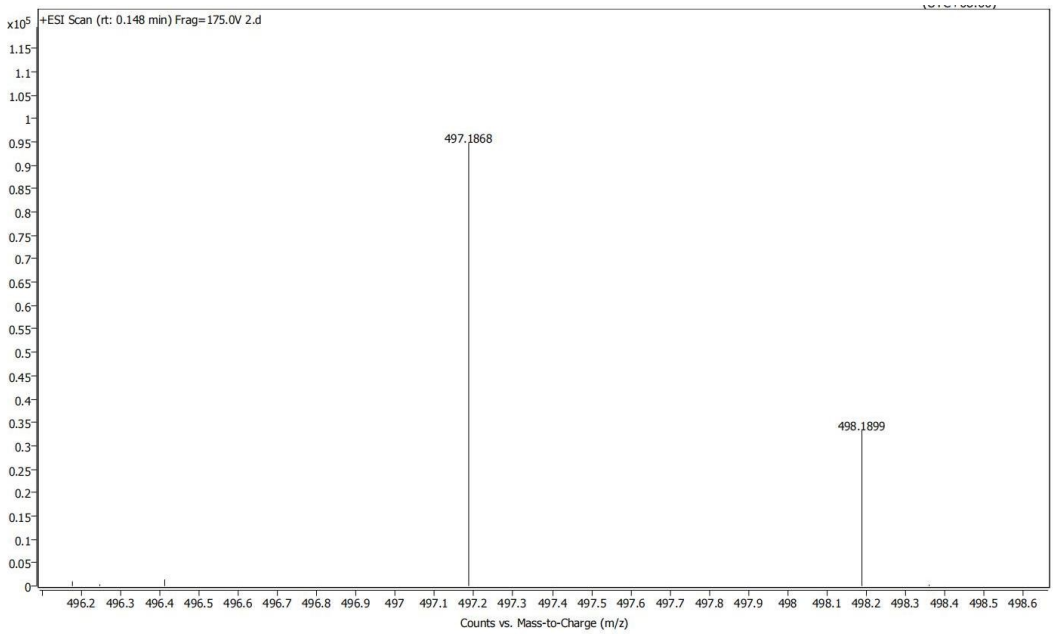

Figure S8. MS spectrum of **TPE-*p*-NO_2P**.

6. NMR Spectra

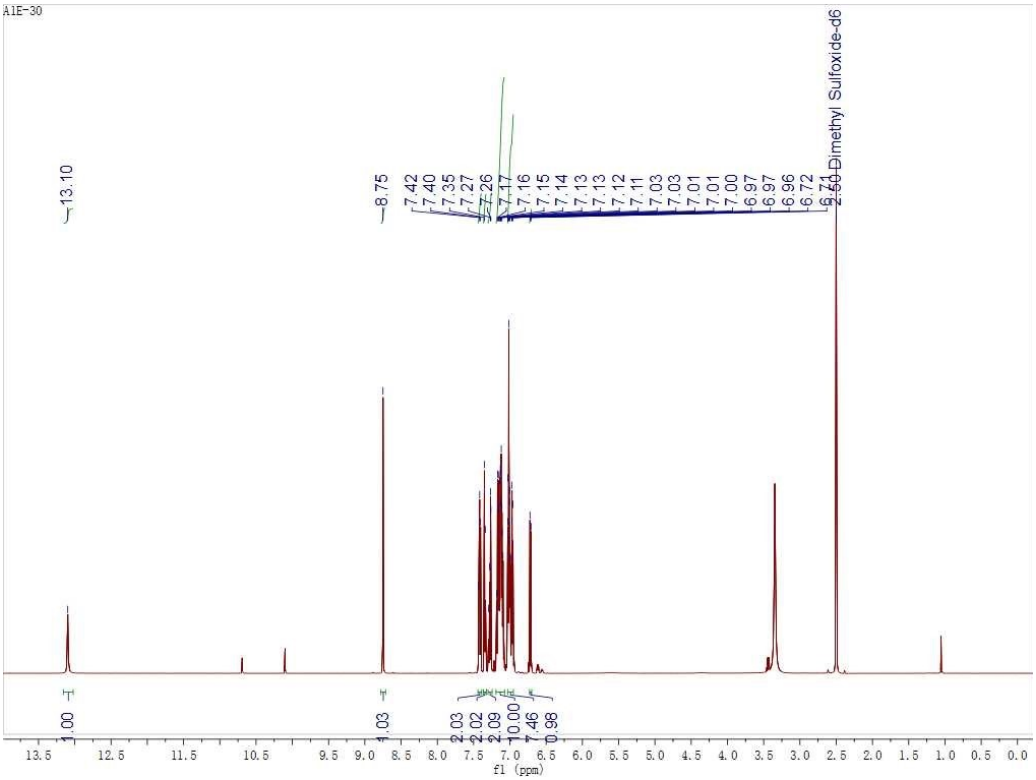

Figure S9. ^{1}H NMR spectrum of **TPE-P**(400 MHz, DMSO-d_6, 298K).

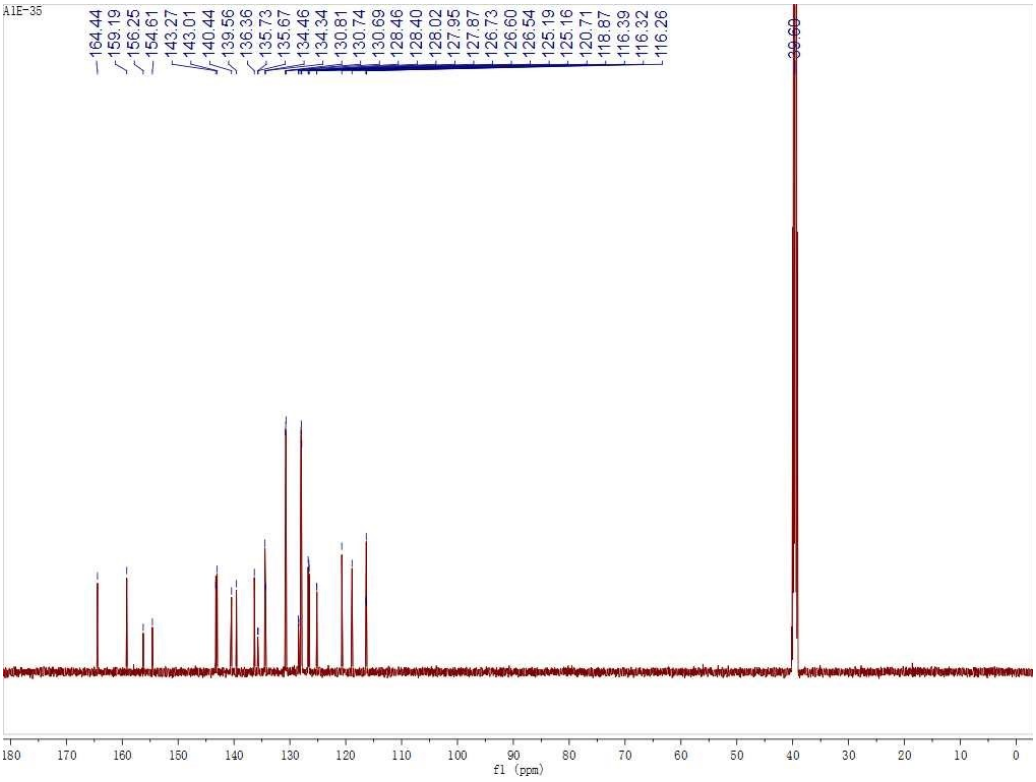

Figure S10. ^{13}C NMR spectrum of **TPE-P**(151 MHz, DMSO-d_6, 298K).

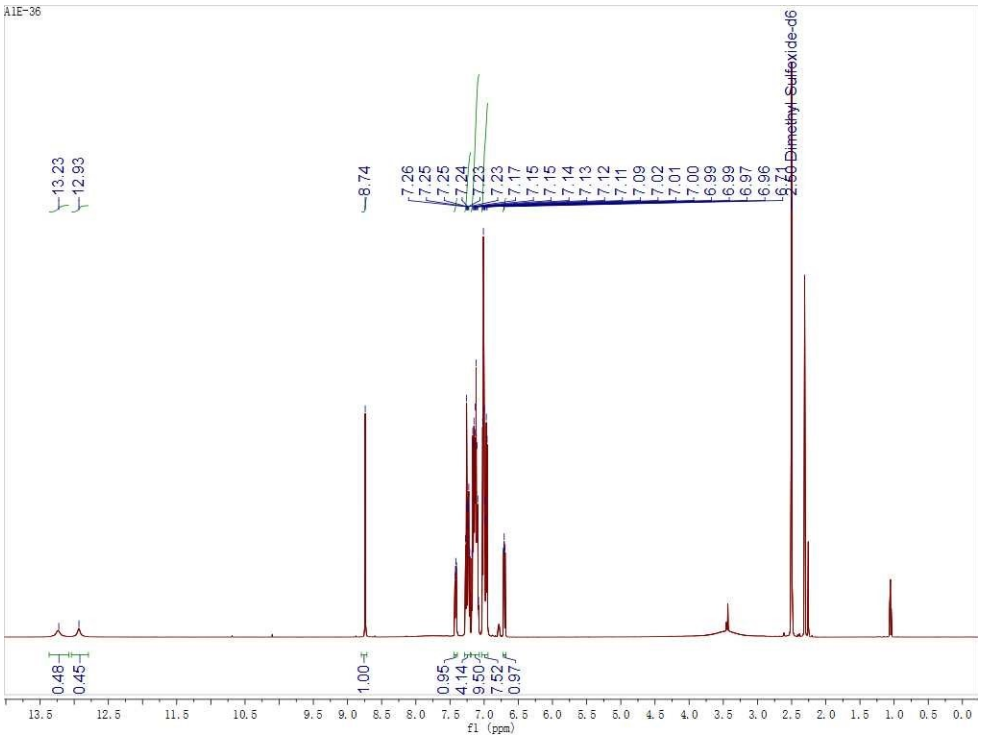

Figure S11. ^{1}H NMR spectrum of **TPE-*o*-FP**(400 MHz, DMSO-d_6, 298K).

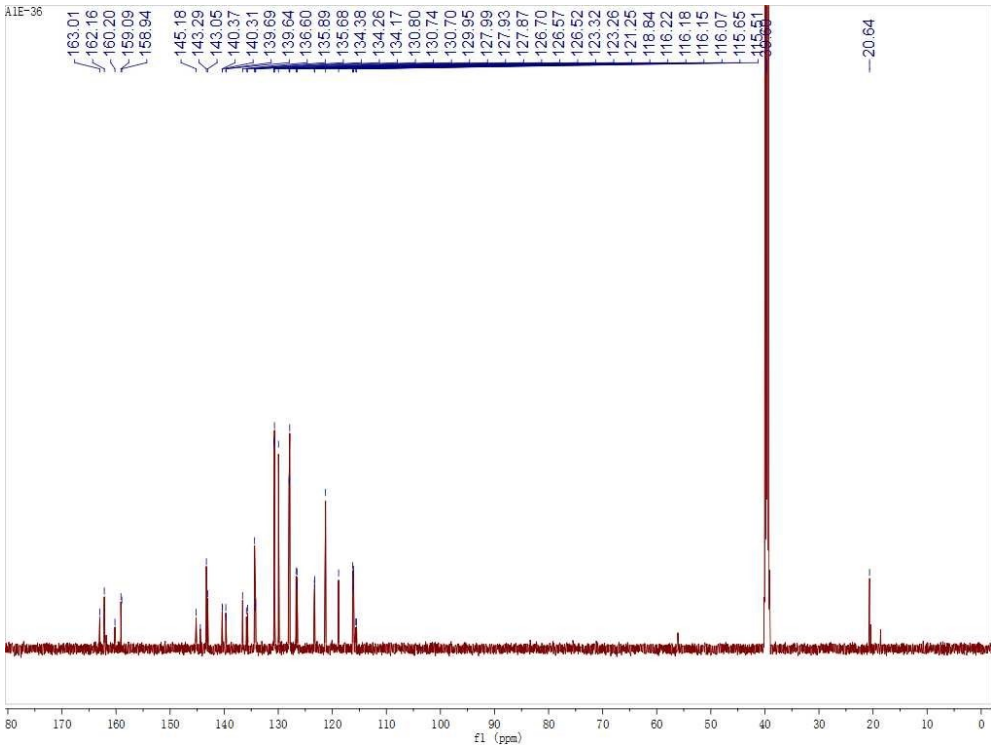

Figure S12. ^{13}C NMR spectrum of **TPE-*o*-FP**(151 MHz, DMSO-d_6, 298K).

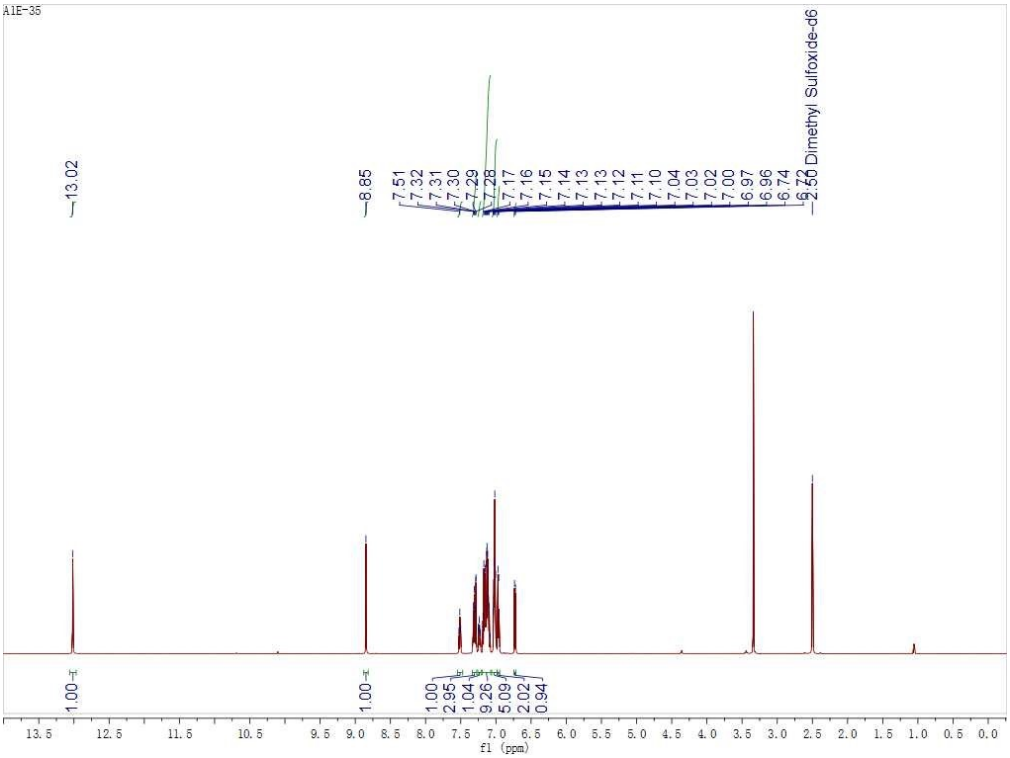

Figure S13. ^{1}H NMR spectrum of **TPE-*p*-FP**(400 MHz, DMSO-d_6, 298K).

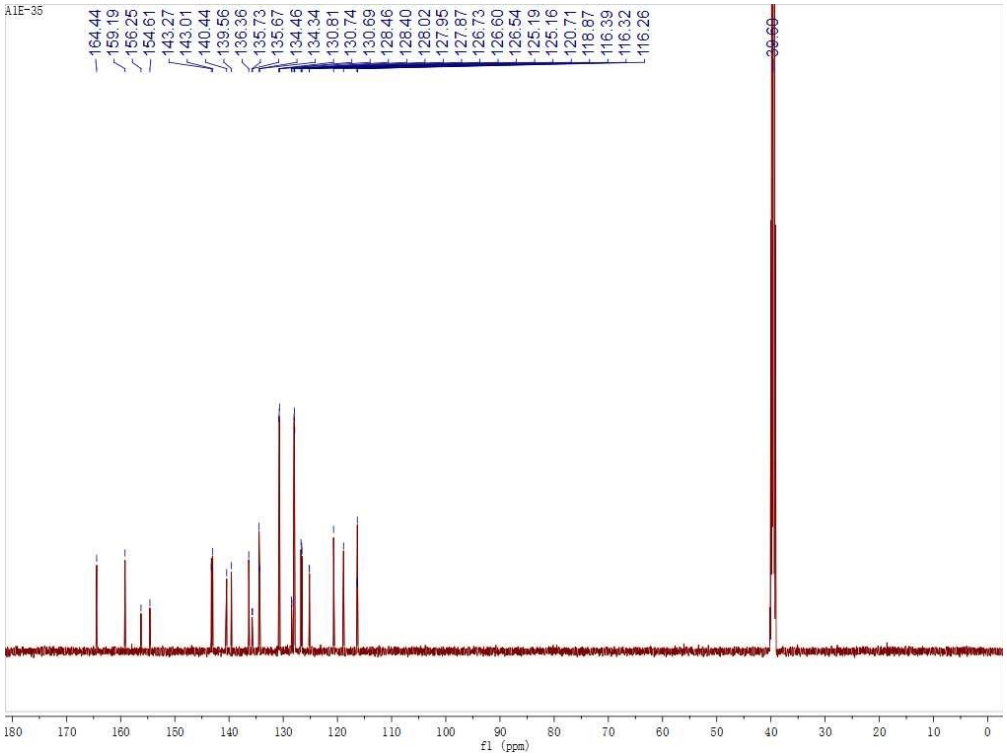

Figure S14. ^{13}C NMR spectrum of **TPE-*p*-FP**(151 MHz, DMSO-d_6, 298K).

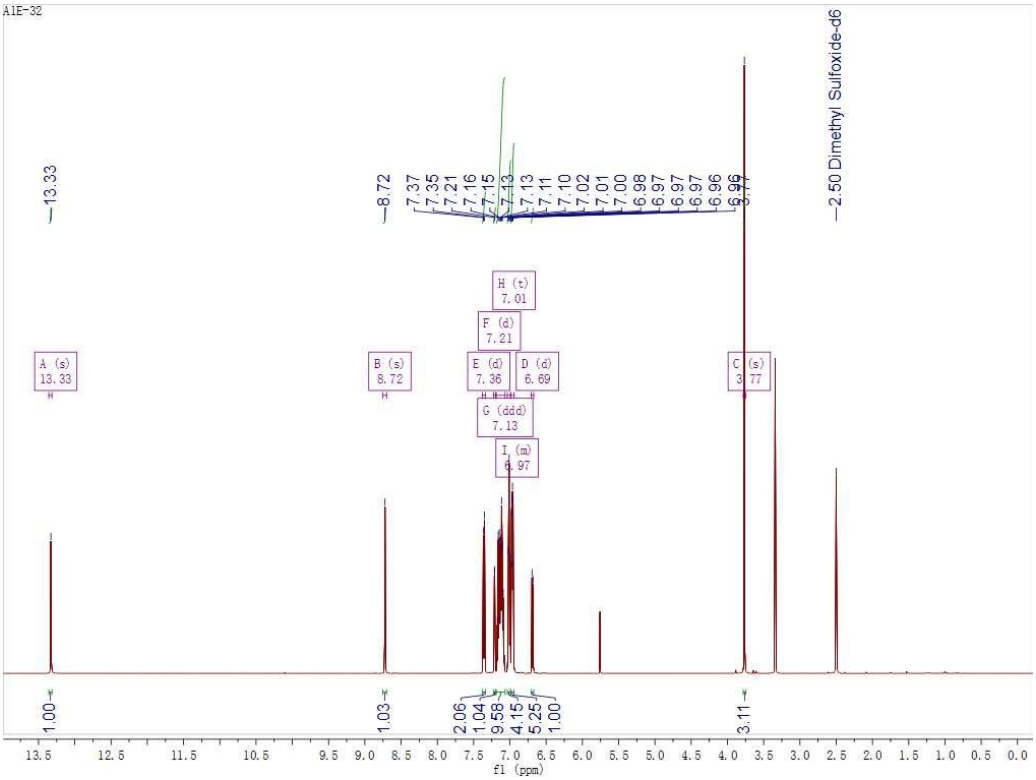

Figure S15. ^{1}H NMR spectrum of **TPE-*p*-MP**(400 MHz, DMSO-d_6, 298K).

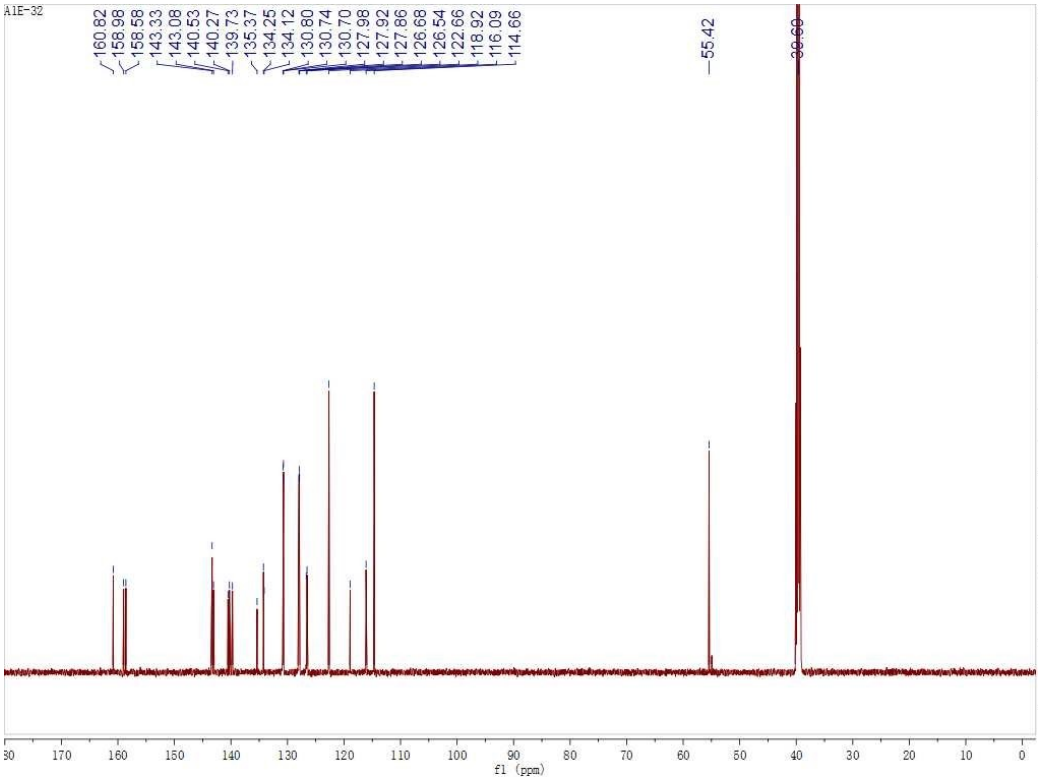

Figure S16. ^{13}C NMR spectrum of **TPE-*p*-MP**(151 MHz, DMSO-d_6, 298K).

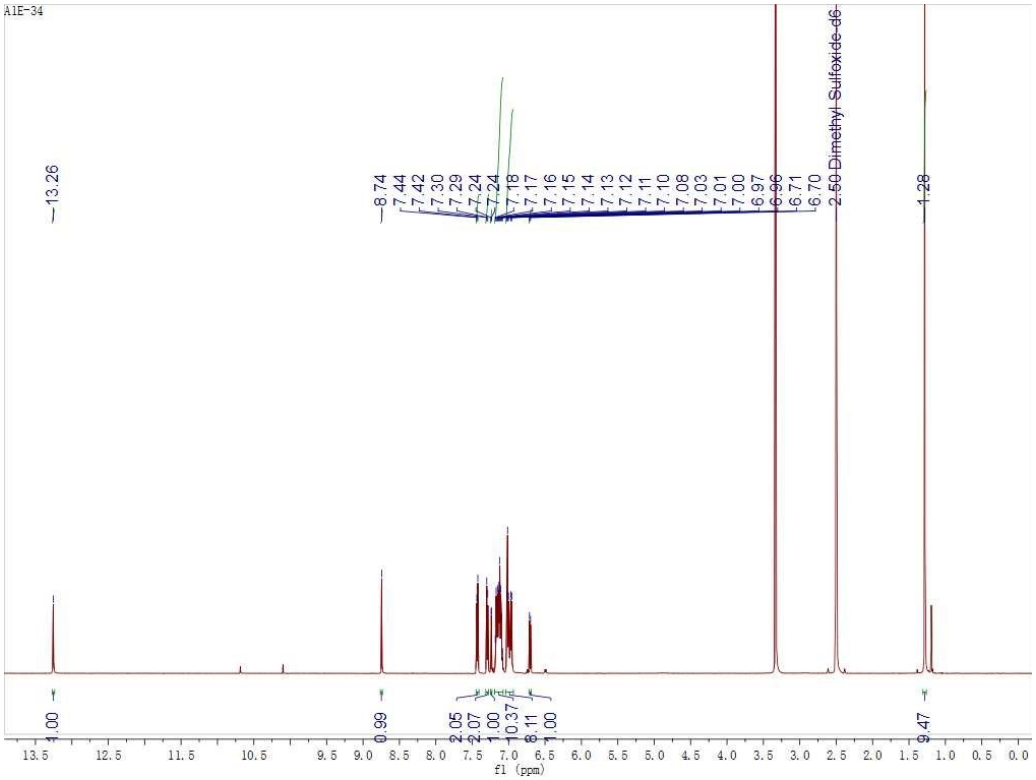

Figure S17. ^{1}H NMR spectrum of **TPE-*p*-tBuP**(400 MHz, DMSO-d_6, 298K).

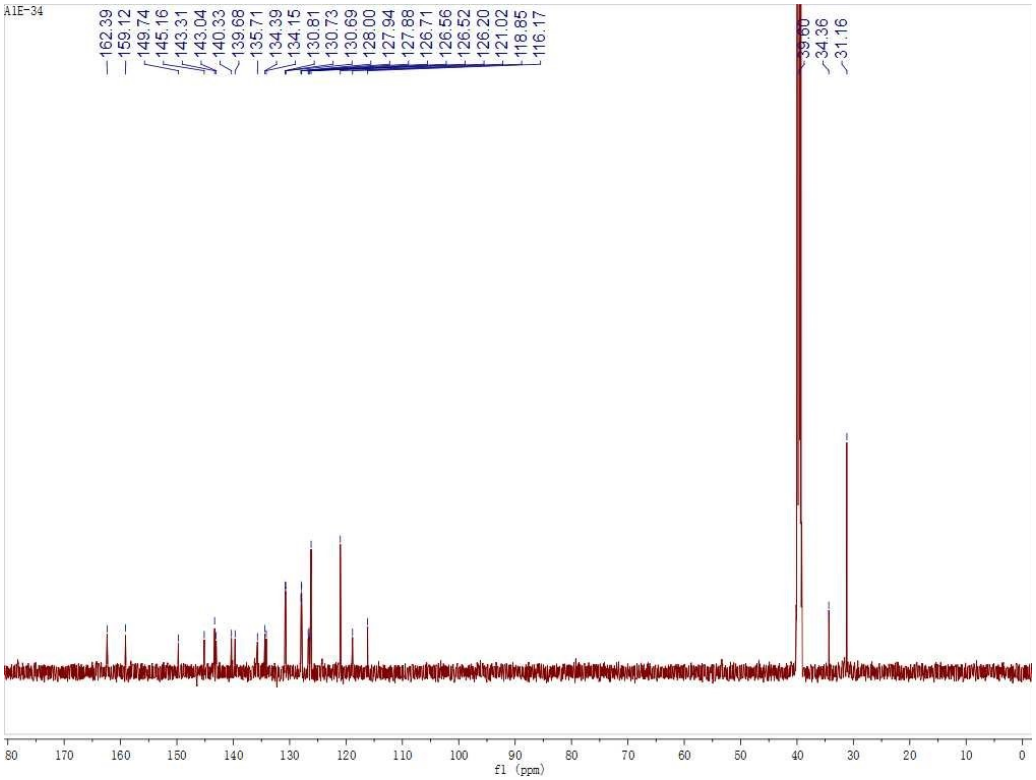

Figure S18. ^{13}C NMR spectrum of **TPE-*p*-tBuP**(151 MHz, DMSO-d_6, 298K).

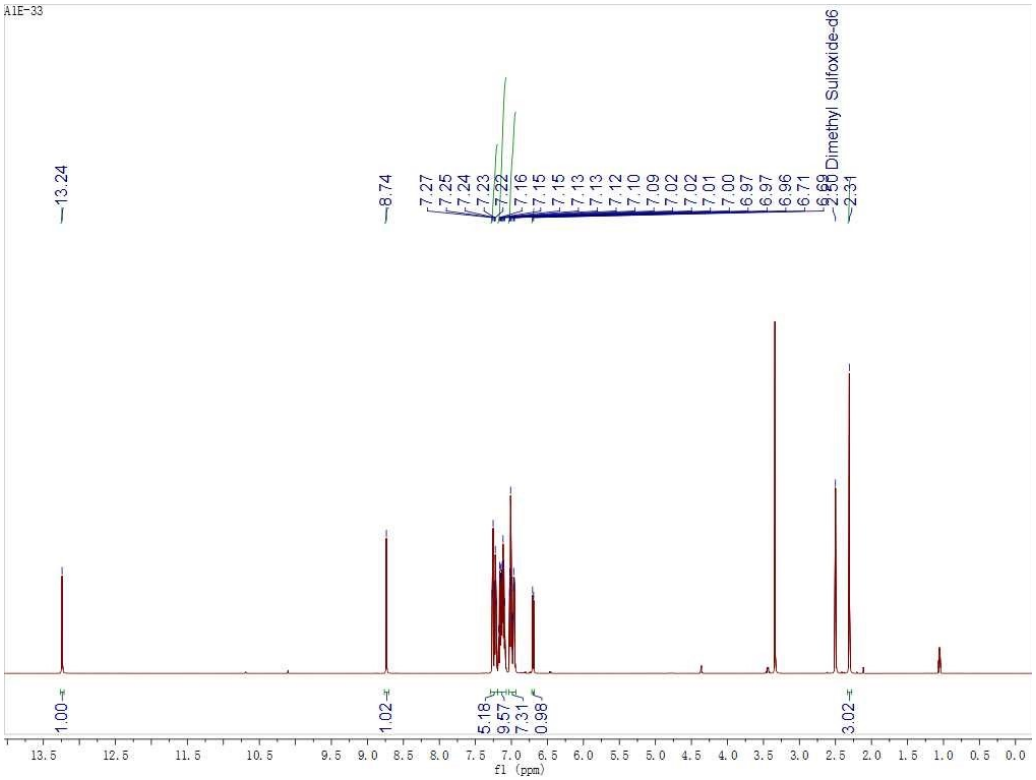

Figure S19. ^{1}H NMR spectrum of **TPE-*p*-MOP**(400 MHz, DMSO-d_6, 298K).

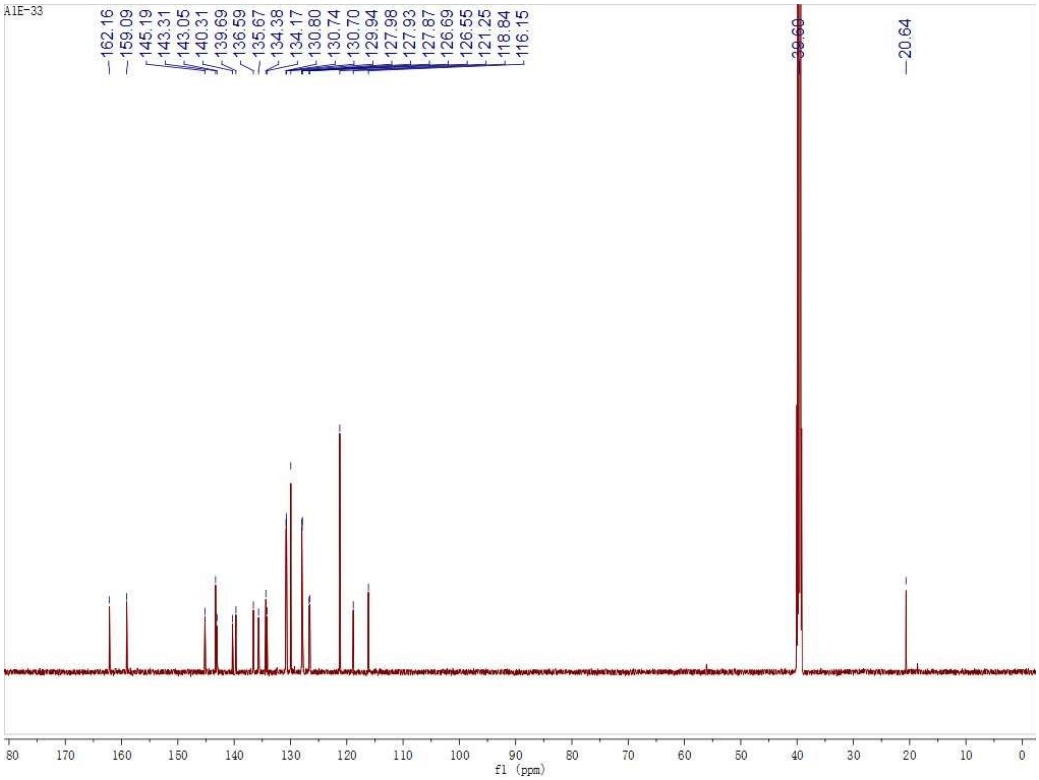

Figure S20. ^{13}C NMR spectrum of **TPE-*p*-MOP**(151 MHz, DMSO-d_6, 298K).

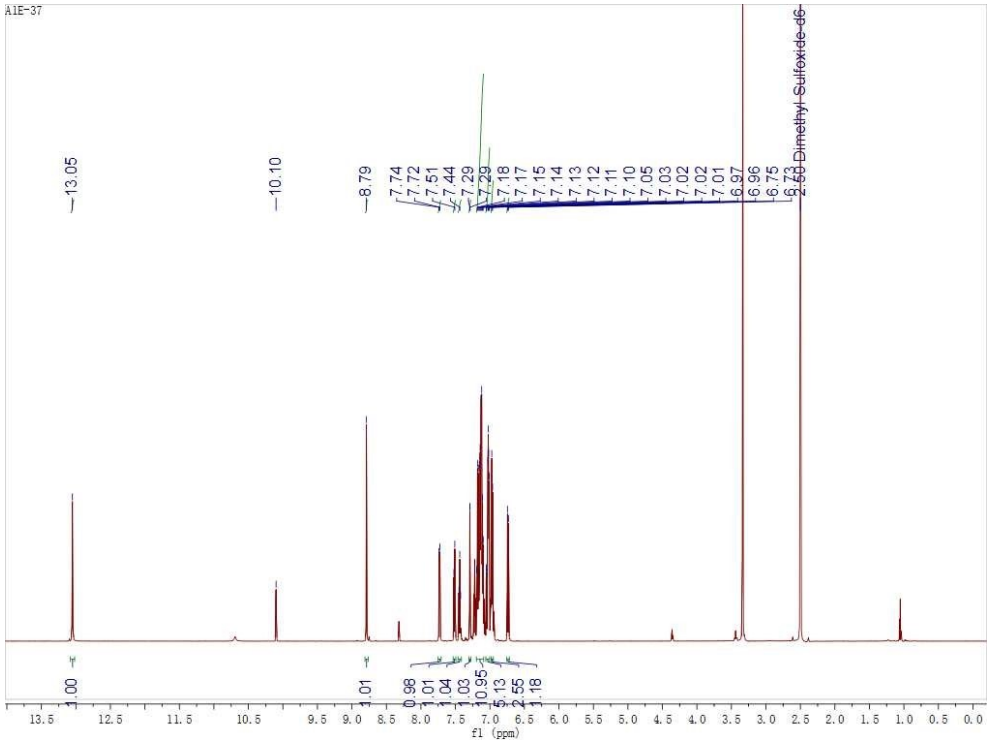

Figure S21. ^{1}H NMR spectrum of **TPE-*o*-BrP**(400 MHz, DMSO-d_6, 298K).

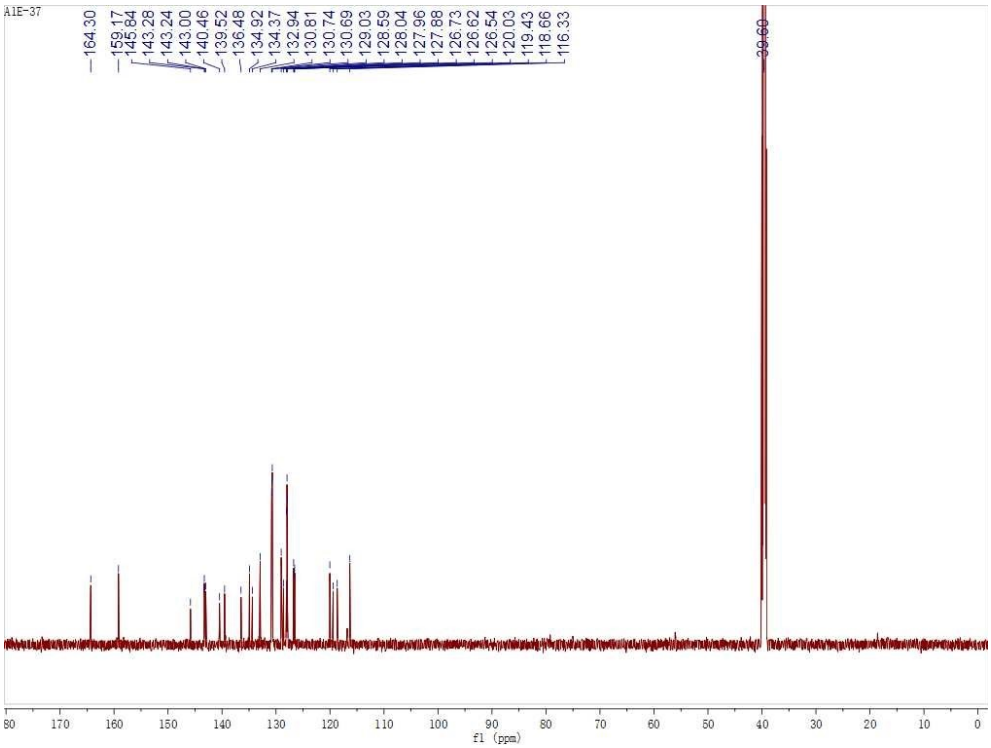

Figure S22. ^{13}C NMR spectrum of **TPE-*o*-BrP**(151 MHz, DMSO-d_6, 298K).

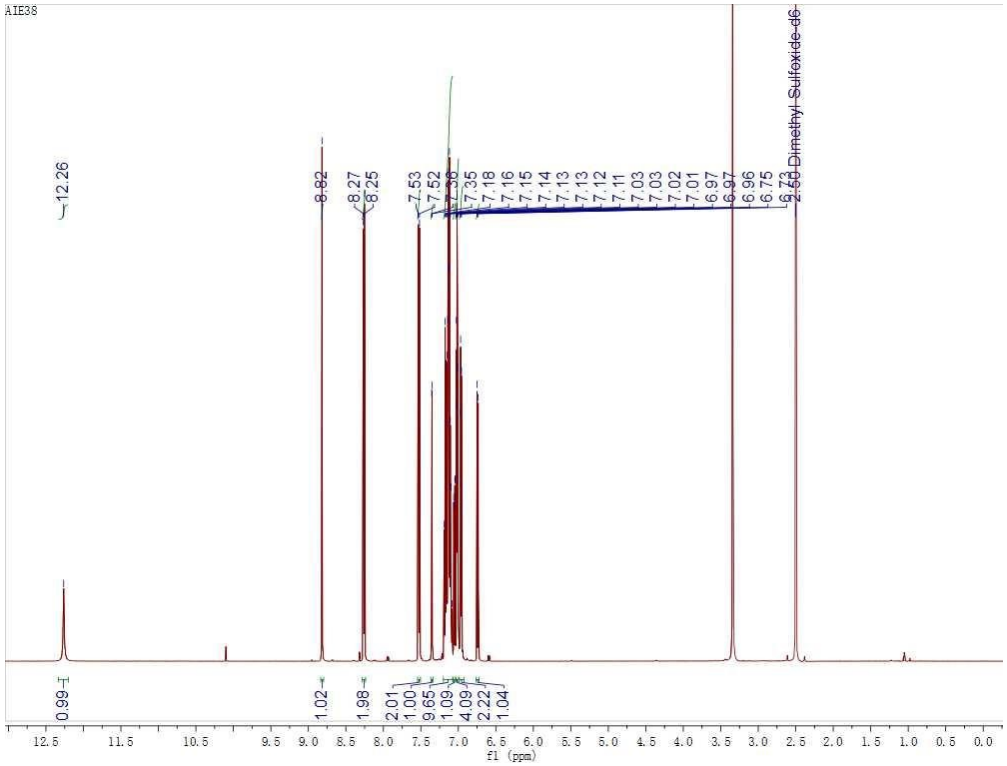

Figure S23. ^{1}H NMR spectrum of **TPE-*p*-NO_2P**(400 MHz, DMSO-d_6, 298K).

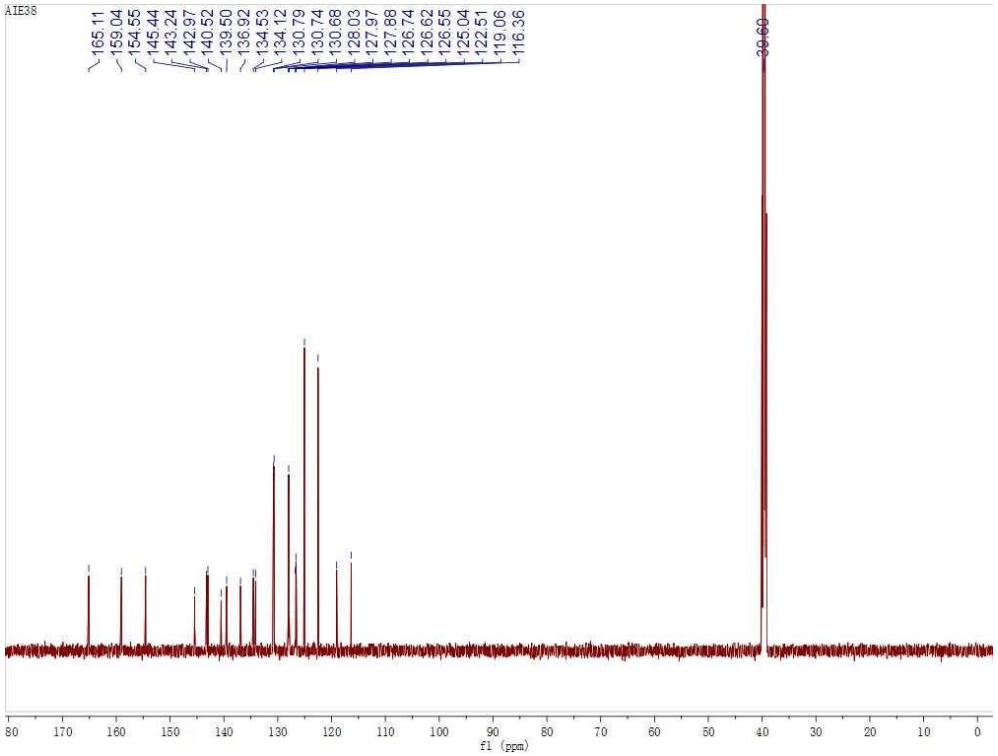

Figure S24. ^{13}C NMR spectrum of **TPE-*p*-NO_2P**(151 MHz, DMSO-d_6, 298K).

7. Supplementary data for spectral analysis

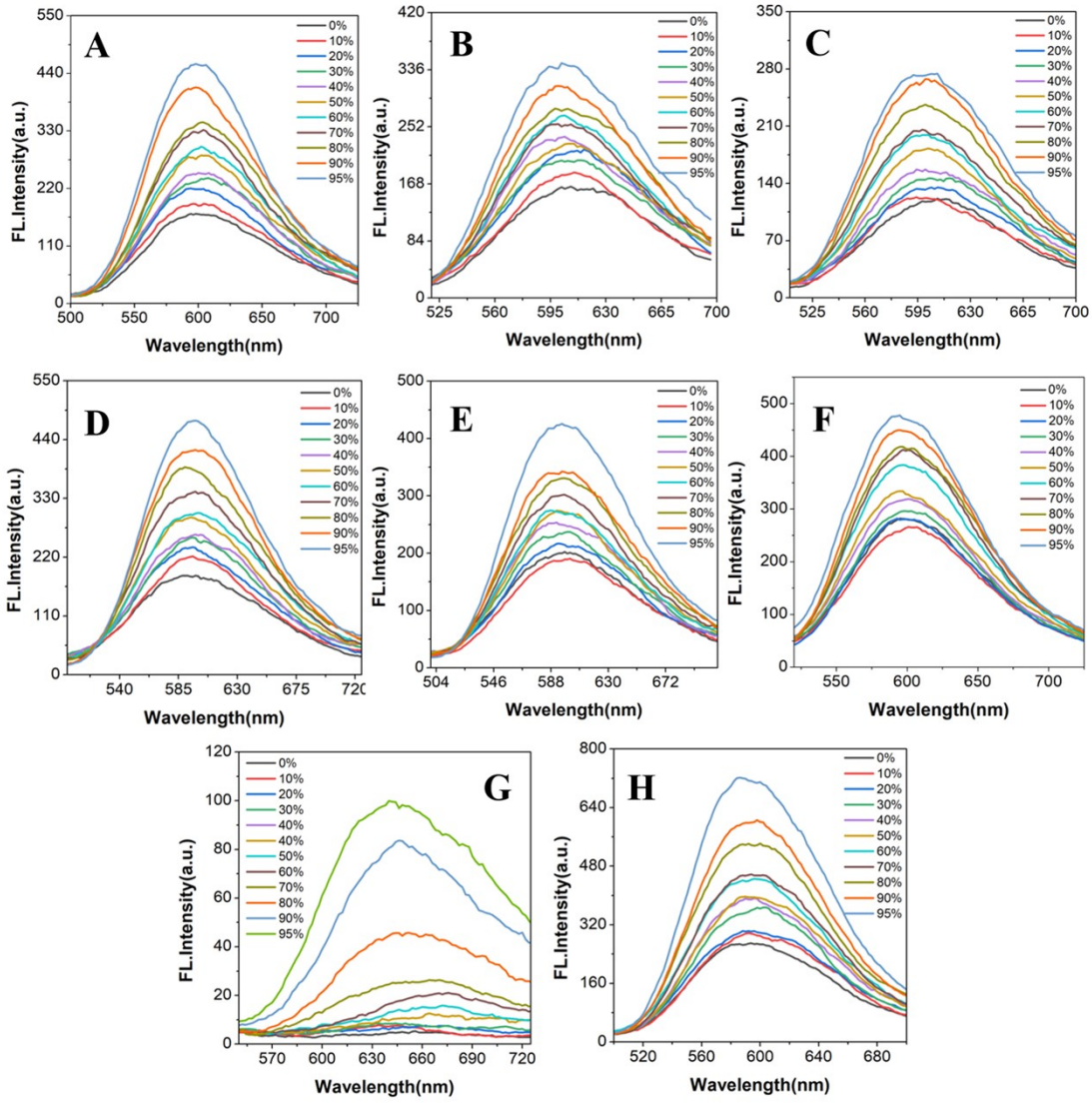

Figure S25. Fluorescence spectra of (A)**TPE-P**, (B)**TPE-*o*-FP**, (C)**TPE-*p*-FP**, (D)**TPE-*p*-MP**, (E)**TPE-*p*-tBuP**, (F)**TPE-*p*-MOP** (G)**TPE-*o*-BrP** and (H)**TPE-*p*-NO_2P** in different ratios of good solvent/poor solvent.

Table S1. Ultraviolet-visible absorption data of the compound.

	TPE-P	**TPE-*o*-FP**	**TPE-*p*-FP**	**TPE-*p*-MP**	**TPE-*p*-tBuP**	**TPE-*p*-MOP**	**TPE-*o*-BrP**	**TPE-*p*-NO_2P**
Wavelength (nm)	314.00	318.00	315.00	321.50	319.00	327.00	310.00	326.00
ε(× 10^4 M^{-1} cm^{-1})	4.40	3.13	5.03	4.91	1.99	3.74	2.64	3.64

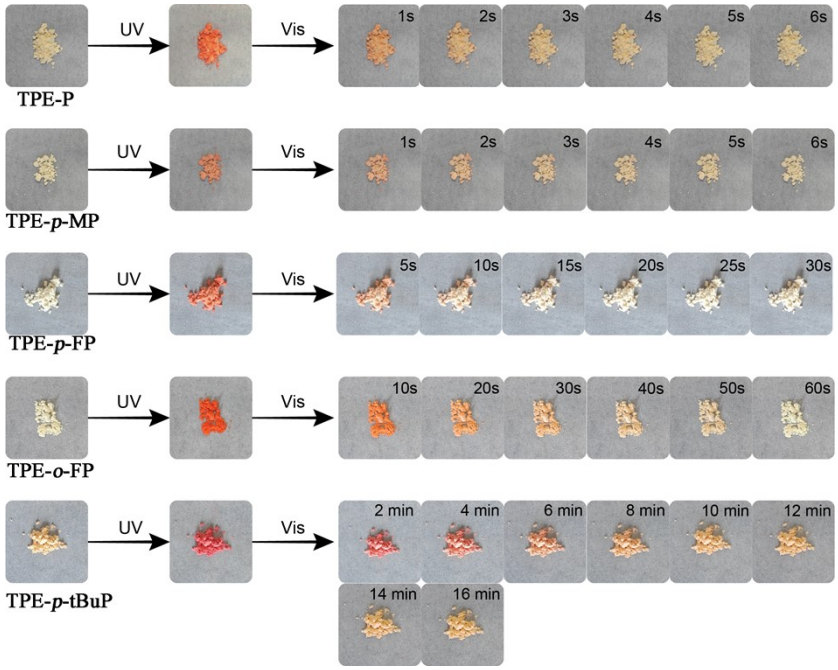

Figure S26. The colour-changing and fading effects of compounds **TPE-P**, **TPE-*p*-MP**, **TPE-*p*-FP**, **TPE-*o*-FP** and **TPE-*p*-tBuP** under ultraviolet excitation.

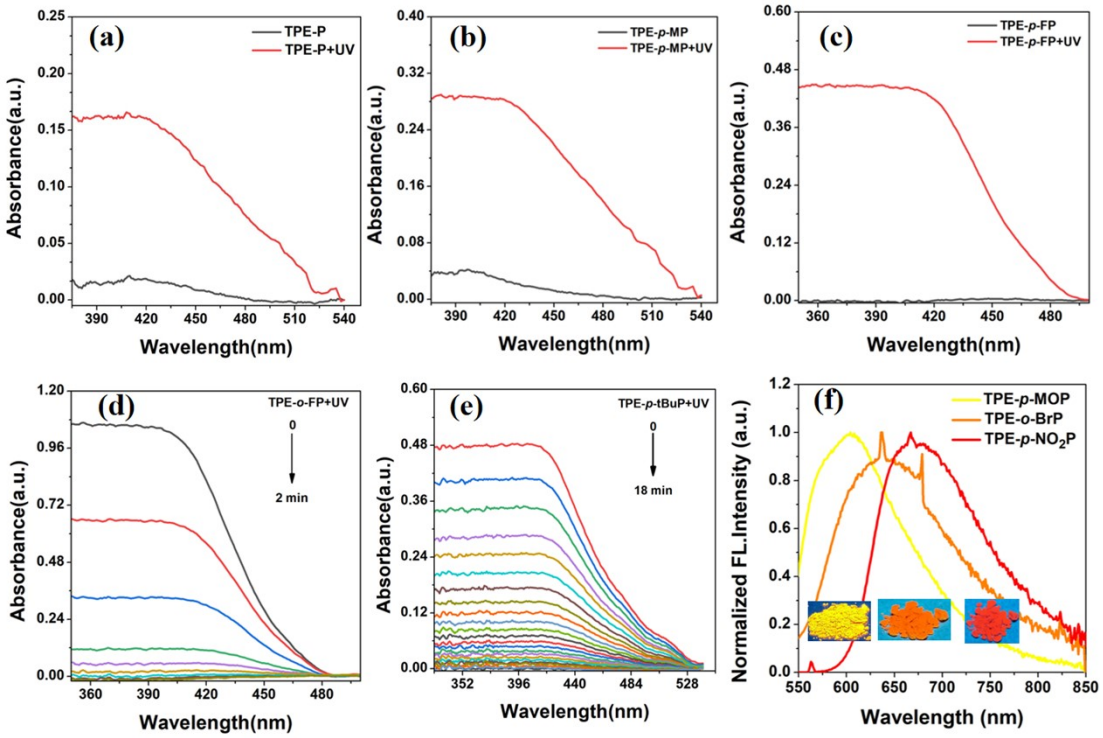

Figure S27. Compounds (a) **TPE-P**, (b) **TPE-*p*-MP**, (c) **TPE-*p*-FP**, (d) **TPE-*o*-FP**, and (e) **TPE-*p*-tBuP** before and after UV excitation, along with (f) solid-state fluorescence spectra of **TPE-*p*-MOP**, **TPE-*o*-BrP** and **TPE-*p*-NO_2P**.

8. Single crystal X-ray diffraction analysis and SEM.

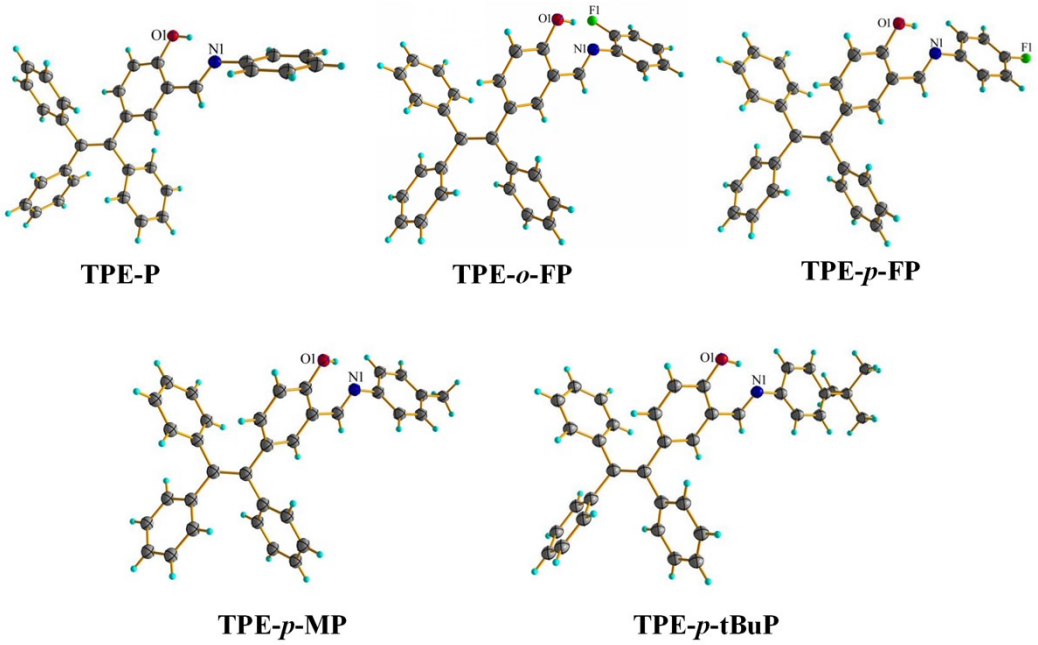

Figure S28. Crystal structure diagrams of **TPE-P**, **TPE-*p*-tBuP**, **TPE-*o*-FP**, **TPE-*p*-FP** and **TPE-*p*-MP**.

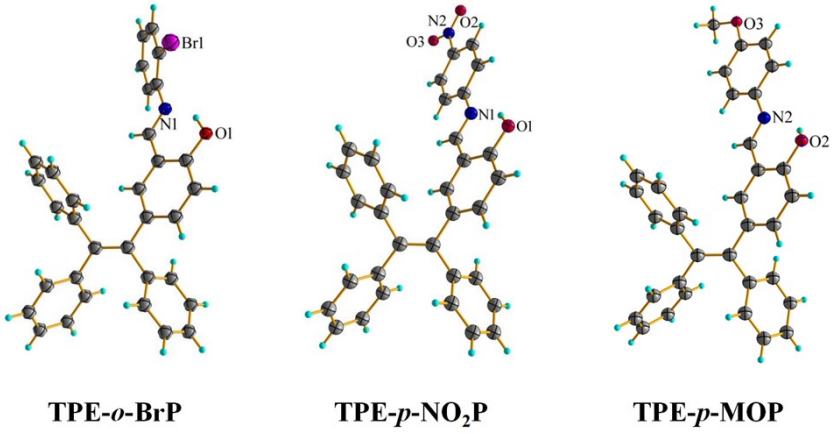

Figure S29. Crystal structure diagrams of **TPE-*p*-MOP**, **TPE-*o*-BrP** and **TPE-*p*-NO_2P**.

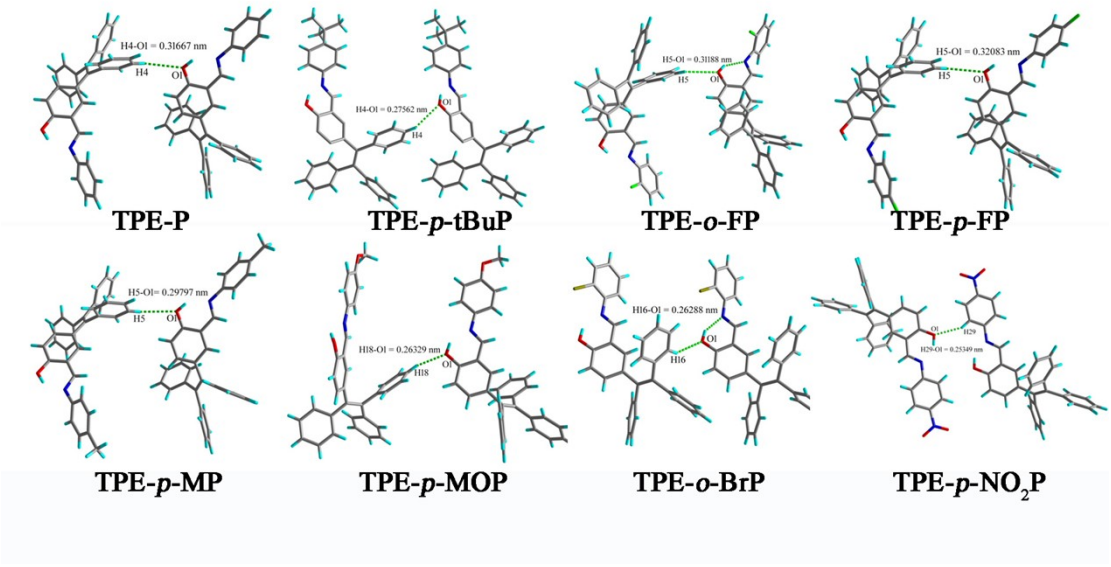

Figure 30. The distance between the hydroxyl group and a carbon atom on another benzene ring in the compound.

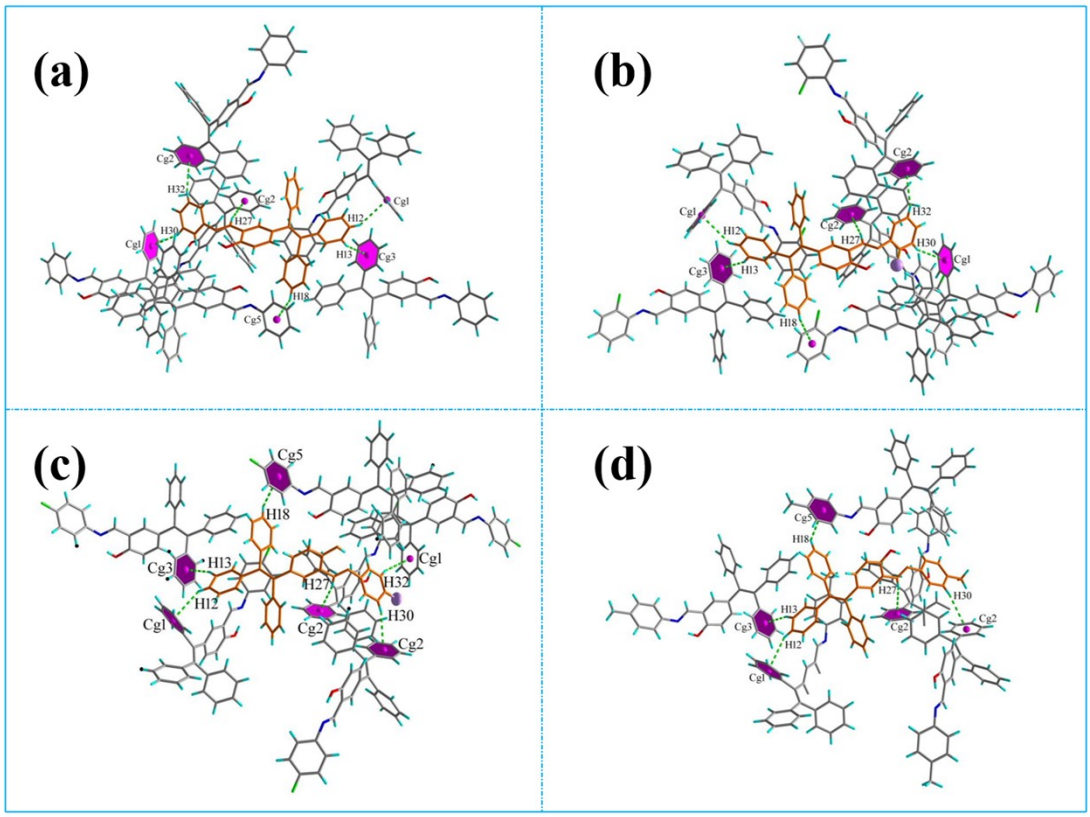

Figure S31. C–H···Cg interactions in (a) **TPE-P**, (b) **TPE-*o*-FP**, (c) **TPE-*p*-FP** and (d) **TPE-*p*-MP**.

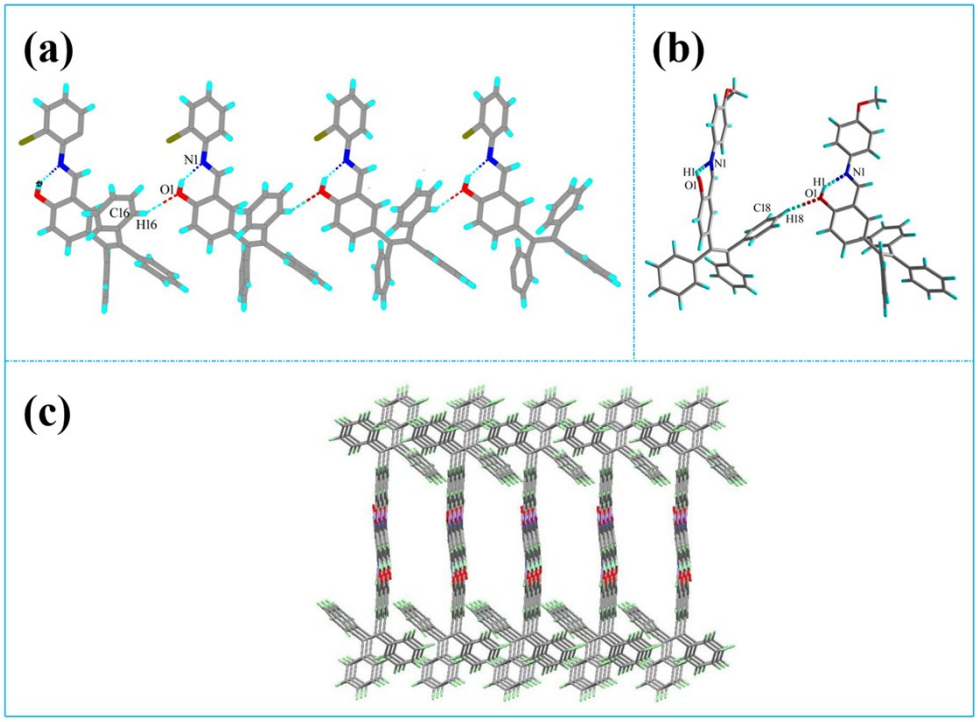

Figure S32. O–H···N hydrogen bonds between molecules of (a) **TPE-*o*-BrP**, (b) **TPE-*p*-MOP** and (c) **TPE-*p*-NO$_2$P** resulting 2D channel networks.

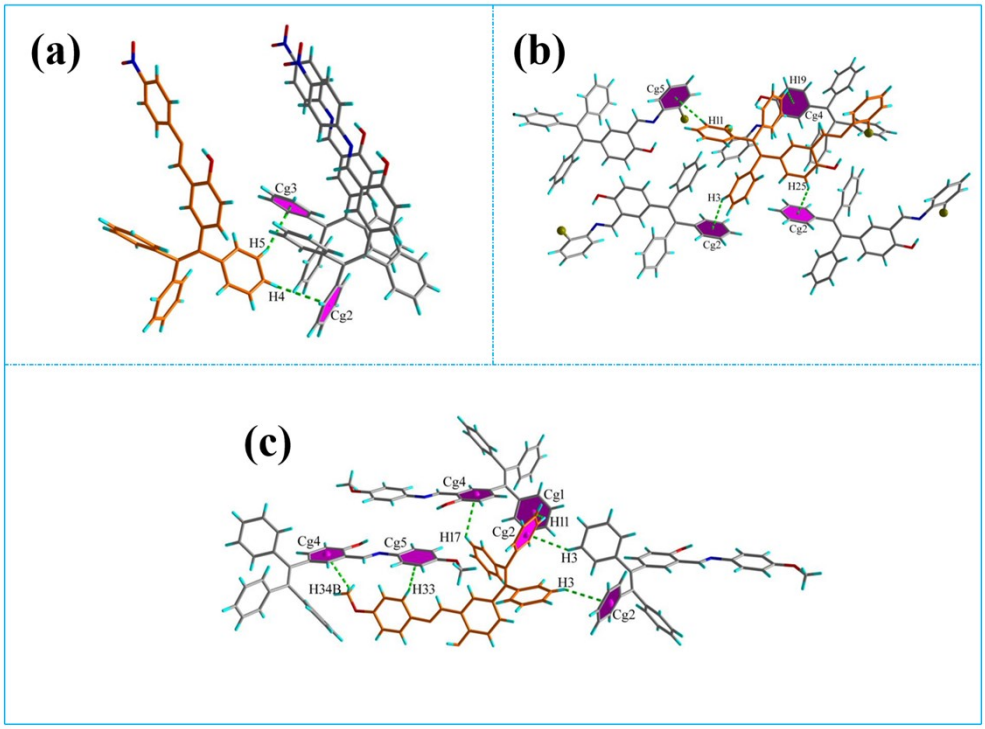

Figure S33. C–H···Cg interactions among (a) **TPE-*p*-NO$_2$P**, (b) **TPE-*o*-BrP** and (c) **TPE-*p*-MOP**.

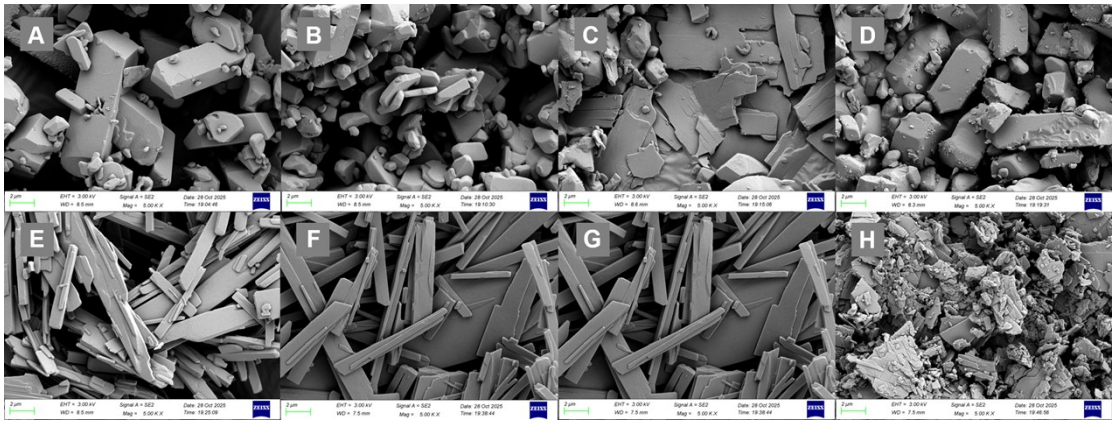

Figure S34. SEM image of the compound in a 2 μm field of view ((A)**TPE-P**, (B) **TPE-*p*-tBuP**, (C) **TPE-*o*-FP**, (D) **TPE-*p*-FP**, (E) **TPE-*p*-MP**, (F) **TPE-*p*-MOP**, (G) **TPE-*o*-BrP** and (H) **TPE-*p*-NO_2P**).

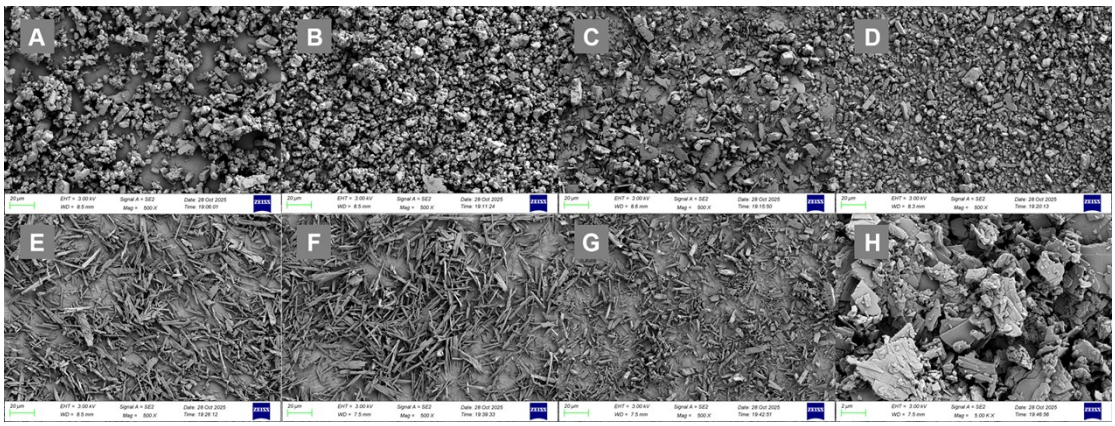

Figure S35. SEM image of the compound in a 20 μm field of view ((A)**TPE-P**, (B) **TPE-*p*-tBuP**, (C) **TPE-*o*-FP**, (D) **TPE-*p*-FP**, (E) **TPE-*p*-MP**, (F) **TPE-*p*-MOP**, (G) **TPE-*o*-BrP** and (H) **TPE-*p*-NO_2P**).

Table S2. X-ray crystallographic parameters of compounds **TPE-P**, **TPE-*o*-FP**, ***TPE-p*-FP** and **TPE-*p*-MP**.

Parameter	**TPE-P**	**TPE-*o*-FP**	**TPE-*p*-FP**	**TPE-*p*-MP**
CCDC	2486844	2486842	2486841	2486845
Empirical formula	$C_{33}H_{25}NO$	$C_{33}H_{24}FNO$	$C_{33}H_{24}FNO$	$C_{34}H_{27}NO$
Formula weight [g mol^{-1}]	451.54	469.53	469.53	465.56
Crystal system	Monoclinic	Monoclinic	Monoclinic	Monoclinic
Space group	$P2_1/n$	$P2_1/n$	$P2_1/n$	$P2_1/n$
a [Å]	10.5319(15)	10.757(2)	10.528(2)	10.657(2)
b [Å]	13.7924(19)	13.767(3)	13.814(3)	14.315(3)
c [Å]	17.028(2)	16.963(3)	17.051(5)	16.926(4)
α	90°	90°	90°	90°
β	92.524(5)	93.487(7)	92.451(9)	92.857(7)
γ	90°	90°	90°	90°
Volume [Å^3]	2471.1(6)	2507.7(9)	2477.5(11)	2578.7(10)
Z	4	4	4	4
Density, calcd [gm^{-3}]	1.214	1.244	1.259	1.199
Temperature [K]	173.00	273.15	273.15	273.15
Unique reflns	3523	3707	2749	3351
Obsd reflns	6039	6192	4813	6364
Parameters	316	326	326	327
R_{int}	0.0775	0.0760	0.0955	0.0950
$R[I>2\sigma(I)]^a$	0.1107	0.0999	0.0730	0.0647
W[all data]R^b	0.1824	0.2349	0.1919	0.1221
GOF on F^2	1.140	1.116	1.045	1.042

Table S3. X-ray crystallographic parameters of compounds **TPE-*p*-tBuP**, **TPE-*o*-BrP**, **TPE-*p*-NO_2P** and **TPE-*p*-MOP**.

Parameter	**TPE-*p*-tBuP**	**TPE-*o*-BrP**	**TPE-*p*-NO_2P**	**TPE-*p*-MOP**
CCDC	2486843	2486846	2486847	2486848
Empirical formula	$C_{37}H_{33}NO$	$C_{33}H_{24}BrNO$	$C_{33}H_{24}N_2O_3$	$C_{34}H_{27}NO_2 \cdot CH_2Cl_2$
Formula weight [g mol^{-1}]	507.64	530.44	496.54	566.49
Crystal system	Triclinic	Triclinic	Triclinic	Monoclinic
Space group	$P\bar{1}$	$P\bar{1}$	$P\bar{1}$	C2/c
a [Å]	6.1709(9)	9.341(4)	5.5572(7)	45.626(2)
b [Å]	9.2484(12)	12.006(4)	9.3767(13)	8.3057(4)
c [Å]	25.973(4)	12.375(5)	25.710(3)	16.4192(8)
α	87.987(5)	100.008(9)	91.759(4)	90
β	88.805(5)	109.515(10)	93.335(4)	90.364(2)
γ	86.401(5)	91.124(11)	102.376(4)	90
Volume [$Å^3$]	1478.2(4)	1283.7(8)	1305.1(3)	6222.0(5)
Z	2	2	2	8
Density, calcd [gm^{-3}]	1.141	1.372	1.264	1.209
Temperature [K]	273.15	273.15	273.15	273.15
Unique reflns	3624	1872	2596	3370
Obsd reflns	5125	6157	6324	6770
Parameters	369	326	344	482
R_{int}	0.0281	0.1698	0.1147	0.0921
$R[I>2\sigma(I)]^a$	0.0984	0.1432	0.1406	0.1347
W[all data]R^b	0.2616	0.2443	0.1886	0.2855
GOF on F^2	1.038	1.018	1.032	1.076

Table S4. Weak intermolecular interaction parameters of photochromism compounds

X-H···Cg	Cg	*d*(H···Cg)/Å	*d*(X···Cg)/Å	X-H···Cg(°)
		TPE-P		
C12-H12···Cg1^{i}	Cg1(C1/C2/C3/C4/C5/C6)	3.0573	3.862(3)	145.65
C13-H13···Cg3^{ii}	Cg3(C15/C16/C17/C18/C19/C20)	2.8036	3.694(4)	160.76
C18-H18···Cg5^{iii}	Cg5(C28/C29/C30/C31/C32/C33)	3.2814	3.832(5)	120.00
C27-H27···Cg2^{iv}	Cg2(C9/C10/C11/C12/C13/C14)	3.0454	3.953(3)	165.52
C30-H30···Cg1^{v}	Cg1(C1/C2/C3/C4/C5/C6)	3.1637	4.042(4)	158.08
C32-H32···Cg2^{vi}	Cg2(C9/C10/C11/C12/C13/C14)	3.2152	4.109(4)	161.50
i=1/2-X,-1/2+Y,1/2-Z,ii=1-X,-Y,-Z,iii=-X,1-Y,-Z,iv=1/2-X,1/2+Y,1/2-Z,v=X,1+Y,Z,vi=-1/2+X,1/2-Y,1/2+Z				
		TPE-*o*-FP		
C12-H12···Cg1^{i}	Cg1(C1/C2/C3/C4/C5/C6)	3.1589	3.932(3)	141.80
C13-H13···Cg3^{ii}	Cg3(C15/C16/C17/C18/C19/C20)	2.8545	3.730(4)	157.32
C18-H18···Cg5^{iii}	Cg5(C28/C29/C30/C31/C32/C33)	3.2587	3.787(5)	118.17
C27-H27···Cg2^{iv}	Cg2(C9/C10/C11/C12/C13/C14)	2.9880	3.903(4)	168.20
C30-H30···Cg1^{v}	Cg2(C9/C10/C11/C12/C13/C14)	3.2041	4.056(5)	153.27
C32-H32···Cg2^{vi}	Cg1(C1/C2/C3/C4/C5/C6)	3.2253	4.099(5)	157.44
i=1/2-X,1/2+Y,1/2-Z,ii=1-X,1-Y,-Z,iii=-X,-Y,-Z,iv=1/2-X,-1/2+Y,1/2-Z,v=-1/2+X,1/2-Y,1/2+Z,vi=X,-1+Y,Z				
		TPE-*p*-FP		
C12-H12···Cg1^{i}	Cg1(C1/C2/C3/C4/C5/C6)	3.0369	3.844(3)	146.04
C13-H13···Cg3^{ii}	Cg3(C15/C16/C17/C18/C19/C20)	2.8239	3.716(4)	161.24
C18-H18···Cg5^{iii}	Cg5(C28/C29/C30/C31/C32/C33)	3.3395	3.891(5)	120.17
C27-H27···Cg2^{iv}	Cg2(C9/C10/C11/C12/C13/C14)	3.0625	3.962(4)	163.34
C30-H30···Cg1^{v}	Cg2(C9/C10/C11/C12/C13/C14)	3.1433	4.035(5)	161.07
C32-H32···Cg2^{vi}	Cg1(C1/C2/C3/C4/C5/C6)	3.2075	4.101(5)	161.77
i=1/2-X,1/2+Y,1/2-Z,ii=1-X,1-Y,-Z,iii=-X,-Y,-Z,iv=1/2-X,-1/2+Y,1/2-Z,v=-1/2+X,1/2-Y,1/2+Z,vi=X,-1+Y,Z				
		TPE-*p*-MP		
C12-H12···Cg1^{i}	Cg1(C1/C2/C3/C4/C5/C6)	3.0773	3.914(3)	150.60
C13-H13···Cg3^{ii}	Cg3(C15/C16/C17/C18/C19/C20)	2.8747	3.770(3)	161.93
C18-H18···Cg5^{iii}	Cg5(C28/C29/C30/C31/C32/C33)	3.2036	3.729(4)	117.75
C27-H27···Cg2^{iv}	Cg2(C9/C10/C11/C12/C13/C14)	3.0995	4.013(3)	167.59
C30-H30···Cg1^{v}	Cg2(C9/C10/C11/C12/C13/C14)	3.3882	4.289(3)	163.70
i=3/2-X,-1/2+Y,1/2-Z,ii=2-X,-Y,-Z,iii=1-X,1-Y,-Z,iv=3/2-X,1/2+Y,1/2-Z,v=-1/2+X,1/2-Y,1/2+Z				
		TPE-*p*-tBuP		
C17-H17···Cg1^{i}	Cg1(C1/C2/C3/C4/C5/C6)	3.0527	3.937(6)	159.39
C36-H36···Cg1^{ii}	Cg1(C1/C2/C3/C4/C5/C6)	3.3815	4.306(14)	162.30
i=X,-1+Y,Z, ii=-X,1-Y,-Z				

Table S5. Weak intermolecular interaction parameters for photoluminescence compounds.

	TPE-*o*-BrP			
C3-H3···Cg2[i]	Cg1(C1/C2/C3/C4/C5/C6)	2.9444	3.759(10)	146.99
C11-H11···Cg5[ii]	Cg5(C28/C29/C30/C31/C32/C33)	3.1695	3.992(10)	148.52
C19-H19···Cg4[iii]	Cg4(C21/C22/C23/C24/C25/C26)	2.9467	3.766(9)	147.72
C25-H25···Cg2[iv]	Cg2(C9/C10/C11/C12/C13/C14)	2.9818	3.752(10)	141.17
i=1-X,2-Y,1-Z, ii=-1+X,1+Y,Z, iii=1-X,1-Y,-Z, iv=1+X,Y,Z				
	TPE-*p*-NO_2P			
C4-H4···Cg2[i]	Cg2(C9/C10/C11/C12/C13/C14)	3.3472	4.111(7)	140.82
C5-H5···Cg3[ii]	Cg3(C15/C16/C17/C18/C19/C20)	3.0158	3.811(8)	144.42
i=X,-1+Y,Z,1/2-Z,ii=-1+X,-1+Y,Z				
	TPE-*p*-MOP			
C3-H3···Cg2[i]	Cg2(C9/C10/C11/C12/C13/C14)	3.1925	3.992(7)	145.24
C11-H11···Cg1[ii]	Cg1(C1/C2/C3/C4/C5/C6)	3.1929	3.793(8)	124.09
C17-H17···Cg4[ii]	Cg4(C21/C22/C23/C24/C25/C26)	3.2657	3.841(8)	122.08
C33-H33···Cg5[iii]	Cg5(C28/C29/C30/C31/C32/C33)	3.3041	4.160(14	153.86
C34-H34···Cg4[iii]	Cg4(C21/C22/C23/C24/C25/C26)	3.1359	3.847(12)	132.22
i=-X,Y,1/2-Z,ii=X,2-Y,1/2+Z,iii=1/2-X,1/2+Y,1/2-Z				

Table S6. The distance and bond angle between the hydroxyl oxygen atom in a compound and the nearest carbon atom and its hydrogen atoms in an adjacent molecule.

Photochromic compounds			**Photoluminescent compounds**		
$d_{C\cdots O}$ (nm)	$d_{O\cdots H}$ (nm)	∠C-H..O(°)	$d_{C\cdots O}$ (nm)	$d_{O\cdots H}$ (nm)	∠C-H..O(°)
	TPE-P			**TPE-o-BrP**	
C4-O1	O1-H4	C4-H4-O1	C16-O1	O1-H16	C16-H16-O1
0.38830	0.31667	133.676	0.34237	0.26288	143.674
	TPE-*o*-FP			**TPE-*p*-NO_2P**	
C5-O1	O1-H5	C5-H5-O1	C29-O1	O1-H29	C29-H29-O1
0.38279	0.31188	134.563	0.33850	0.25349	152.105
	TPE-*p*-FP			**TPE-*p*-MoP**	
C5-O1	O1-H5	C5-H5-O1	C18-O1	O1-H18	C18-H18-O1
0.39145	0.32083	134.239	0.34875	0.26329	152.747
	TPE-*p*-MP				
C5-O1	O1-H5	C5-H5-O1			
0.37509	0.29797	141.223			
	TPE-*p*-tBuP				
C4-O1	O1-H4	C5-H4-O1			
0.036186	0.27562	154.778			

9. Theoretical calculation data

Table S7. Molecular frontier orbital energy levels for the enol form, ketone form, and anti-ketone form of the compound.

	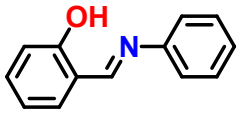			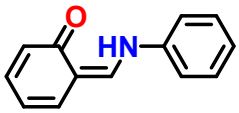			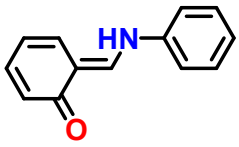		
	E_{HOMO}	E_{LUMO}	ΔE	E_{HOMO}	E_{LUMO}	ΔE	E_{HOMO}	E_{LUMO}	ΔE
TPE-P	-0.20501	-0.07567	0.12937	-0.19411	-0.08966	0.10445	-0.19412	-0.09225	0.10187
TPE-*o*-FP	-0.20611	-0.07982	0.12629	-0.1958	-0.09287	0.10293	-0.196	-0.09543	0.10057
TPE-*p*-FP	-0.20706	-0.07898	0.12808	-0.19635	-0.09201	0.10434	-0.19642	-0.09464	0.10178
TPE-*p*-MP	-0.2038	-0.0734	0.1304	-0.19216	-0.08717	0.10499	-0.19197	-0.08995	0.10202
TPE-*p*-tBuP	-0.20356	-0.07324	0.13032	-0.19184	-0.08673	0.10511	-0.19169	-0.08958	0.10211
TPE-*o*-BrP	-0.20692	-0.07977	0.12715	-0.19716	-0.09163	0.10553	-0.19787	-0.09522	0.10265
TPE-*p*-NO_2P	-0.21185	-0.08432	0.12753	-0.20192	-0.10269	0.09923	-0.20252	-0.10309	0.09943
TPE-*p*-MOP	-0.20316	-0.07128	0.13188	-0.1918	-0.08379	0.10801	-0.19116	-0.08765	0.10351

† ΔE=E_{LUMO}-E_{HOMO}, Units are eV.

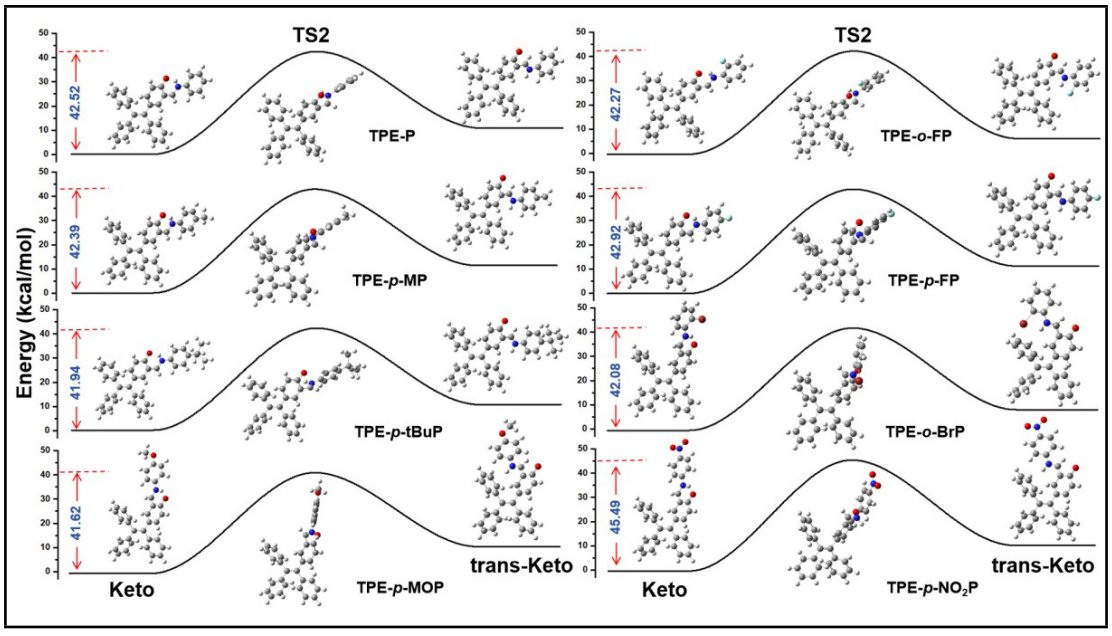

Figure S36. Energy profiles of the keto-to-trans-keto isomerization in TPE derivatives and their corresponding optimized geometries.

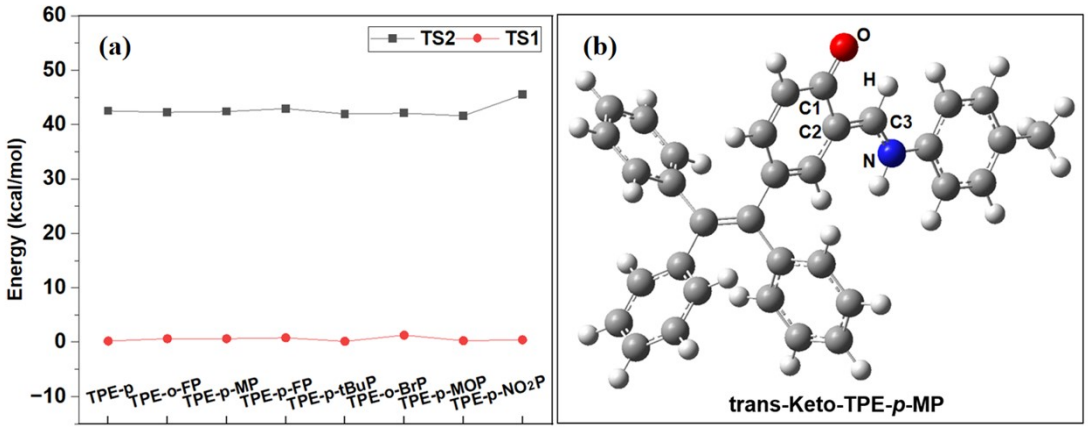

Figure S37. (a) Energy barriers for enol-to-keto (TS1) and keto-to-trans-keto (TS2) isomerization; (b) enlarged view of **TPE-P**.

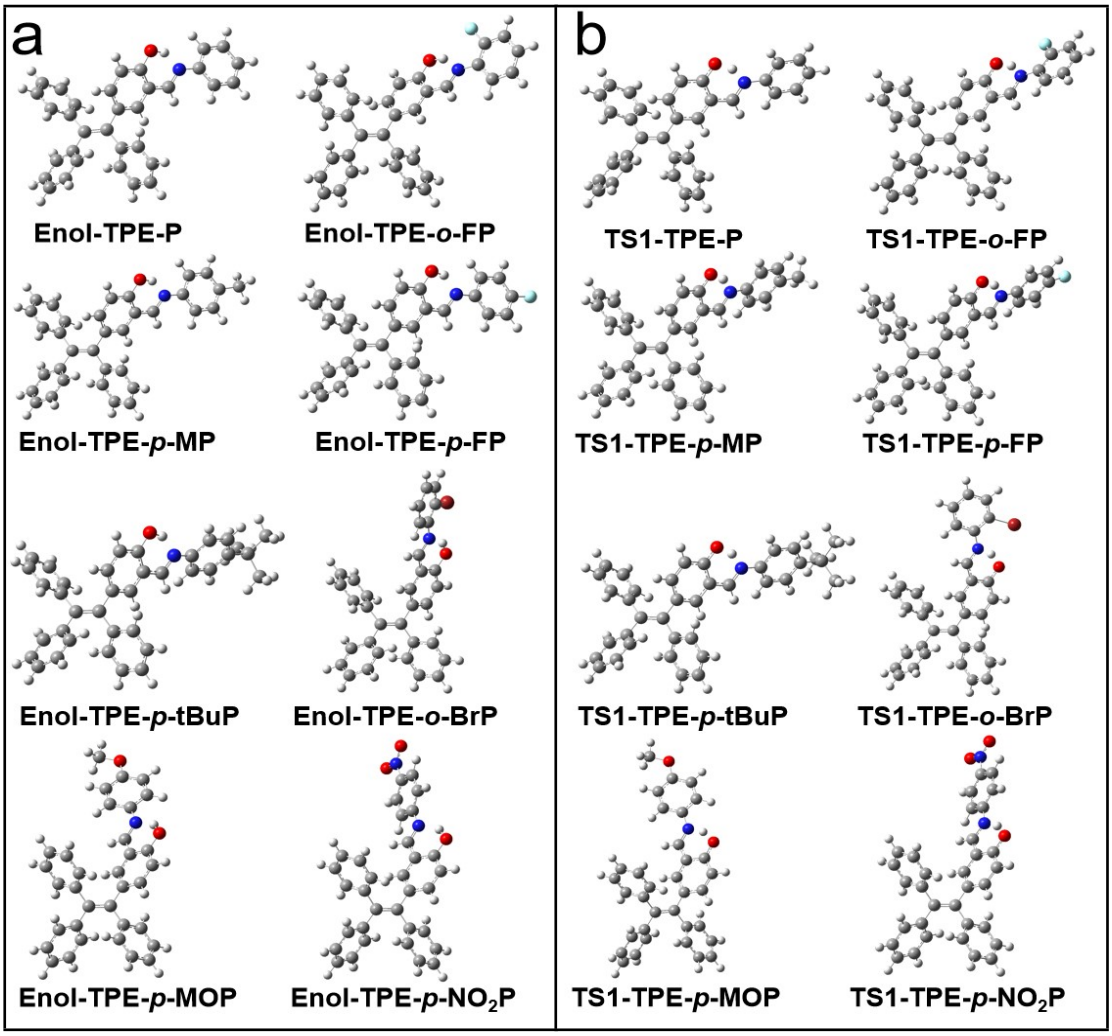

Figure S38. The optimized structures of (a) enol and (b) the transition states (TS1) from enol to keto for a series of TPE derivatives.

Table S8. The selected bond lengths (Å) and angles of the involved structures during enol-to-keto conversion and the reaction energy barriers of TS1 (E_{TS1}, kcal/mol).

system	bond length	**TPE-P**	**TPE-*o*-FP**	**TPE-*p*-MP**	**TPE-*p*-FP**	**TPE-*p*-tBuP**	**TPE-*o*-BrP**	**TPE-*p*-MOP**	**TPE-*p*-NO_2P**
Enol	H-O	1.020	1.018	1.021	1.018	1.021	1.015	1.020	1.016
	O-C1	1.361	1.359	1.361	1.361	1.361	1.358	1.361	1.360
	C1-C2	1.425	1.427	1.425	1.425	1.425	1.427	1.425	1.427
	C2-C3	1.447	1.444	1.447	1.446	1.447	1.444	1.448	1.441
	C3-N	1.305	1.305	1.305	1.306	1.305	1.304	1.305	1.309
	N-H	1.671	1.680	1.668	1.678	1.666	1.708	1.669	1.688
TS1	H-O	1.229	1.240	1.229	1.236	1.228	1.250	1.256	1.228
	O-C1	1.330	1.325	1.330	1.329	1.330	1.323	1.330	1.327
	C1-C2	1.443	1.445	1.443	1.444	1.443	1.445	1.443	1.446
	C2-C3	1.426	1.421	1.427	1.425	1.427	1.420	1.428	1.419
	C3-N	1.321	1.324	1.320	1.322	1.320	1.325	1.320	1.328
	N-H	1.262	1.255	1.262	1.255	1.264	1.249	1.256	1.262
Keto	H-O	1.678	1.707	1.676	1.667	1.677	1.710	1.665	1.676
	O-C1	1.293	1.288	1.294	1.293	1.294	1.288	1.295	1.290
	C1-C2	1.466	1.468	1.465	1.466	1.495	1.467	1.464	1.470
	C2-C3	1.401	1.397	1.402	1.400	1.402	1.396	1.404	1.395
	C3-N	1.341	1.345	1.340	1.342	1.340	1.345	1.338	1.349
	N-H	1.048	1.046	1.048	1.049	1.048	1.047	1.050	1.048
E_{TS1}	---	0.21	0.64	0.64	0.79	0.15	1.28	0.27	0.42

Table S9. The selected bond lengths (Å) and dihedral angles (°) of the involved structures during keto-to-trans-keto conversion and the reaction energy barriers of TS2 (E_{TS2}, kcal/mol).

system	bond length / dihedral Angle	**TPE-P**	**TPE-*o*-FP**	**TPE-*p*-MP**	**TPE-*p*-FP**	**TPE-*p*-tBuP**	**TPE-*o*-BrP**	**TPE-*p*-MOP**	**TPE-*p*-NO_2P**
Keto	C2-C3	1.401	1.397	1.402	1.400	1.402	1.396	1.404	1.395
	C3-N	1.341	1.345	1.340	1.342	1.340	1.345	1.338	1.349
	C1-C2-C3-N	-0.272	0.309	-0.277	-0.269	-0.268	0.032	-0.240	-0.097
TS2	C2-C3	1.465	1.464	1.465	1.465	1.465	1.464	1.465	1.464
	C3-N	1.316	1.321	1.315	1.318	1.315	1.320	1.314	1.327
	C1-C2-C3-N	-84.857	-84.146	-85.060	-84.384	-85.109	-83.813	-84.531	-83.397
trans-keto	C2-C3	1.385	1.382	1.386	1.384	1.386	1.382	1.387	1.379
	C3-N	1.354	1.357	1.353	1.356	1.353	1.356	1.353	1.364
	C1-C2-C3-N	178.596	-179.813	178.592	178.316	178.619	178.078	-173.187	-173.198
E_{TS2}	---	42.52	42.27	42.39	42.92	41.94	42.08	41.62	45.49